

Base Station Cooperation with Feedback Optimization: A Large System Analysis

Rusdha Muharar, Randa Zakhour and Jamie Evans

Abstract

In this paper, we study feedback optimization problems that maximize the users' signal to interference plus noise ratio (SINR) in a two-cell MIMO broadcast channel. Assuming the users learn their direct and interfering channels perfectly, they can feed back this information to the base stations (BSs) over the uplink channels. The BSs then use the channel information to design their transmission scheme. Two types of feedback are considered: analog and digital. In the analog feedback case, the users send their unquantized and uncoded CSI over the uplink channels. In this context, given a user's fixed transmit power, we investigate how he/she should optimally allocate it to feed back the direct and interfering (or cross) CSI for two types of base station cooperation schemes, namely, Multi-Cell Processing (MCP) and Coordinated Beamforming (CBf). In the digital feedback case, the direct and cross link channel vectors of each user are quantized separately, each using RVQ, with different size codebooks. The users then send the index of the quantization vector in the corresponding codebook to the BSs. Similar to the feedback optimization problem in the analog feedback, we investigate the optimal bit partitioning for the direct and interfering link for both types of cooperation.

We focus on regularized channel inversion precoding structures and perform our analysis in the large system limit in which the number of users per cell (K) and the number of antennas per BS (N) tend to infinity with their ratio $\beta = \frac{K}{N}$ held fixed. We show that for both types of cooperation, for some values of interfering channel gain, usually at low values, no cooperation between the base stations is preferred: This is because, for these values of cross channel gain, the channel estimates for the cross link are not accurate enough for their knowledge to contribute to improving the SINR and there is no benefit in doing base station cooperation under that condition. We also show that for the MCP scheme, unlike in the perfect CSI case, the SINR improves only when the interfering channel gain is above a certain threshold.

The material in this paper was presented in part at the IEEE International Conference on Communications (ICC), Ottawa, Canada, June 2012 and at the IEEE International Symposium on Information Theory (ISIT), Cambridge, MA, USA, July 2012.

Rusdha Muharar is with the Department of Electrical and Computer Systems Engineering, Monash University, Clayton, VIC 3800, Australia and Syiah Kuala University, Banda Aceh, Indonesia (e-mail: rusdha.muharar@monash.edu; r.muharar@unsyiah.ac.id).

Randa Zakhour is part-time faculty at the Schools of Engineering of the American University of Science and Technology and of the Lebanese International University, Lebanon (email: randa.zakhour@gmail.com).

Jamie Evans is with the Department of Electrical and Computer Systems Engineering, Monash University, Clayton, VIC 3800, Australia (email: jamie.evans@monash.edu).

I. INTRODUCTION

A. Background

Recently, many applications that require high data rates such as high quality video streaming and huge volume data transfers through wireless communication systems have emerged. MIMO communication systems have arisen as a promising candidate to support this requirement and have been adopted for existing and future wireless communication standards such as in IEEE 802.11n and 4G networks. Current MIMO technological advancements can be considered as the results of research works started about fifteen years ago. So far, there has been a considerable amount of work focusing on single user and single-cell multiuser MIMO systems. Only recently, researchers have started to put more attention to investigate how to maximize data rates in *multi-cell* MIMO networks, particularly in the downlink [1, and references therein].

The main challenge that limits the spectral efficiency in the downlink of multi-cell networks, besides intra-cell interference, is the inter-cell interference (ICI). The conventional approach to mitigate this interference is to use spatial reuse of resources such as frequency and time [1]. The move towards aggressive frequency or time reuse will cause the networks to be interference limited especially for the users at the cell edge. The current view is to mitigate ICI through base station (BS) cooperations. Within this scheme, the BSs share the control signal, channel state information (CSI) and data symbols for all users via a central processing unit or wired backhaul links [2].

It has been established in [3]–[8], to name a few, that MIMO cooperation schemes provide a significant increase in spectral efficiency compared to conventional cellular networks. BS cooperation can be implemented at different levels [1]. In the *Multi-Cell Processing* setup, also known as *Network MIMO* or *Coordinated Multi-Point* (CoMP) transmission, the BSs fully cooperate and share both the channel state information (CSI) and transmission data. This full cooperation requires high capacity backhaul links which are sometimes not viable in practical settings. To alleviate this requirement, only CSI (including direct and interfering channels) is shared amongst base stations in the *interference coordination* scheme [1]. Several works have addressed coordinated beamforming and power control schemes to improve the spectral efficiency in interference-limited downlink multi-cell networks. Detailed discussions regarding these topics can be found in [1] and references therein.

In both base station cooperation schemes, the CSI at the base stations plays an important role in maximizing the system performance. The base stations use this information to adapt their transmission strategies to the channel conditions. The benefit of having CSI at the transmitter (CSIT) with respect to the capacity in single and multi-cell multi-antenna systems is nicely summarized in [9], [10]. However, these advantages are also accompanied by the overhead cost for the CSI acquisition via channel training and feedback in frequency division duplex (FDD) systems. It needs to scale proportionally to the number of transmit and receive antennas and the number of users in the system in order to maintain a constant gap of the sum-rate with respect to the full CSI case [11]. Moreover, in practical systems, the backhaul-link capacity for CSI and user data exchanges and feedback-link bandwidth are limited [2]. Considering the CSI signaling overhead from channel training and CSI feedback, references [12], [13]

(see also [14]) suggested that the conventional single-cell processing (SCP) without coordination may outperform the cooperative systems, even the MCP scheme. In this paper, to reduce the complexity in the analysis, we ignore the (important) constraints of limited backhaul-link and CSI training overhead. We assume a perfect CSI training so that all users know their CSI perfectly. We focus on studying how to allocate feedback resources, that depend on the feedback schemes, to send the CSI for the direct channel and interfering (cross) channel to BSs so that the users' SINR are maximized. Two feedback schemes are considered in our study: the analog feedback scheme, introduced in [15] and the limited (quantized) feedback via random vector quantization (RVQ), introduced in [16]. In the analog feedback scheme, each user sends its unquantized and uncoded channel state information through the uplink channel. Hence, we ask the question, for a given uplink power constraint, what fraction of this uplink power is allocated optimally to transmit the direct and interfering channel information? For the digital feedback scheme, the number of feedback bits determines the quality of the CSI. Hence, we can ask, how many bits are optimally needed to feedback the direct and cross CSI?

B. Contributions

The main goal of this paper is to optimize and investigate the effect of feedback for MCP and CBf cooperation schemes under analog and quantized feedback (via RVQ). We consider a *symmetric* two-cell Multi-Input Single-Output (MISO) network where the base stations have multiple antennas and each user has a single antenna. We assume that the users in each cell know their own channel perfectly: they feed back this information through the uplink channel and the base stations form the users' channel estimates. The BSs use these estimates to construct a regularized channel inversion (RCI) type beamformer, also called regularized zero-forcing (RZF), to precode the data symbols of the users. The precoders follow the structures proposed in [17]. Unlike [2], [14], we assume several users are simultaneously active in each cell so that the users experience both intra- and inter-cell interference. To mitigate ICI through base station cooperation, we consider both full cooperation (MCP) and interference coordination via CBf.

Our contributions can be summarized as follows. First, under both feedback models and both cooperation schemes, we derive the SINR expression in the large system limit, also called the *limiting SINR*, where the number of antennas at base stations and the number of users in each cell go to infinity with their ratio kept fixed: As our numerical results will show, *this is indicative of the average performance for even finite numbers of antennas*. Then, we formulate a joint optimization problem that performs the feedback optimization for both feedback models and both cooperation schemes and finds the optimal regularization parameter of the corresponding RCI-structured precoder. The regularization parameter is an important design parameter for the precoder because it controls the amount of interference introduced to the users. Optimizing this parameter, as discussed later, will allow the precoder to adapt to the changes of the CSIT quality and consequently produces a '*robust beamformer*'.

We analyze the behavior of the maximum limiting SINR as a function of the cross channel gains and the available feedback resources, and identify, for both the analog and quantized feedback models, regions where SCP

processing is optimal. We also show that whereas in the perfect CSI case, MCP performance always improves with epsilon, this only occurs after a certain threshold is crossed in both analog and limited feedback cases.

Parts of this work appeared in [18], [19], but without the proofs.

C. Related Works

In the last decade, there has been a large volume of research discussing feedback schemes in multi-antenna systems. A summary of digital feedback (also known as limited or finite-rate feedback) schemes in multi-antenna (also single-antenna) and multi-user systems in the single-cell setup can be found in [11]. Since the optimal codebook for the limited feedback is not known yet [16], [20], [21], the use of RVQ, which is based on a random codebook, as the feedback scheme becomes popular. Furthermore, the RVQ-based system performance analysis is also more tractable. In multiple-antenna and multiuser systems, works on the analog feedback commonly refer to [15] (sometimes [22]).

The paper by Jindal [20] sparked the use of RVQ in analyzing broadcast channels. Considering a MISO broadcast channel with a zero-forcing (ZF) precoder and assuming that each user knows its own channel, the main result in the paper is that the feedback rate should be increased linearly with the signal-to-noise ratio (SNR) to maintain the full multiplexing gain. Caire et al. in [21] investigate achievable ergodic sum rates of BC with ZF precoder under several practical scenarios. The CSI acquisition involves four steps; downlink training, CSI feedback, beamformer selection and dedicated training where each user will try to estimate the coupling between its channel and the beamforming vectors. They derive and compare the lower bound and upper bound of the achievable ergodic sum-rate of the analog feedback as in [15] and RVQ-based digital feedback under different considerations, e.g., feedback transmission over AWGN and MAC channel, feedback delay and feedback errors for the digital feedback scheme. A subsequent work by Kobayashi et al. in [23] studies training and feedback optimizations for the same system setup as in [21] except without dedicated training. The optimal period for the training and feedback that minimized achievable rate gap (with and without perfect CSI) are derived under different scenarios as in [21]. The authors also show that the digital feedback can give a significant advantage over the analog feedback. In the same spirit as [20], reference [24] discusses the feedback scaling (as SNR increases) in order to maintain a constant rate gap for a broadcast channel with RCI precoder. The analysis has been done in the large system limit since the analysis the finite-size turns out to be difficult [20]. Moreover, besides analyzing for the case $K = N$, as in [20], the authors also investigate the case $K < N$.

While channel state feedback in the single-cell system has received a considerable amount of attention so far, fewer works have addressed this problem in multi-cell settings. The effect of channel uncertainty, specifically the channel estimation error, in the multi-cell setup is studied in [25], [26]. In [26], the authors conclude that when channel estimates at one base station contain interferences from the users in other cells, also called as pilot contamination phenomenon, the inter-cell interference increases. Thus, this phenomenon could severely impact the performance of the systems. Huh et al. in [25] investigate optimal user scheduling strategies to reduce the

feedback and also the effects of channel estimation error on the ergodic sum-rate of the clustered Network MIMO systems. They consider the ZF precoder at the base stations and derive the optimal power allocation that maximizes the weighted sum-rate. In deriving the results, it is assumed that the BSs received perfectly (error-free) the CSI fed back by the users. The overhead caused by the channel training is also investigated and they observe that there is a trade-off between the number of cooperating antennas and the cost of estimating the channel. Based on the trade-off, the optimal cooperation cluster size can be determined. By incorporating the channel training cost, no-coordination amongst the base stations could be preferable. The same conclusion is also obtained in [12], [13].

For the interference coordination scheme, [2] presents the RVQ-based limited feedback in an infinite Wyner cellular model using generalized eigenvector beamforming at the base stations. The work adopts the intra-cell TDMA mechanism where a single user is active in each cell per time slot. Each user in each cell is also assumed to know its downlink channel perfectly. Based on that system model, an optimal bit partitioning strategy for direct and interfering channels that minimizes the sum-rate gap is proposed. Explicitly, it is a function of the received SNR from the direct and cross links. It is observed that as the received SNR from the cross link increases, more bits are allocated to quantize the cross channel. A better quality of the cross channel estimate will help to reduce the inter-cell interference. The authors also show that the proposed bit partitioning scheme reduces the average sum-rate loss. Also in the interference coordination setting, [14] takes into account both CSI training and feedback in analyzing the system what they called the inter-cell interference cancellation (ICIC) scheme. In ICIC, the precoding vector of a user is the projection of its channel in the null-space of the others users' channels in other cells so that the transmission from this user will not cause interference to the users in other cells. The work also assumes the intra-cell TDMA and presents the training optimization and feedback optimization for both analog and digital feedback (RVQ). Based on that system setup, the most interesting result is that the training optimization is more important than the feedback optimization for the analog feedback while the opposite holds for the digital feedback.

For different levels of cooperation, i.e., MCP, CBf and SCP, [17] investigates an optimization problem to minimize the total downlink transmit power while satisfying a specified SINR target. The authors derived the optimal transmit power, beamforming vectors, cell loading and achieved SINR for those different cooperation schemes in a symmetric two-cell network. The resulted optimal beamforming vectors have a structure related to RCI.

The current work is closely related to [17] in the sense we use the same cooperative schemes and precoder structure. We extend the work by analyzing the optimal feedback strategies for analog and digital feedback under MCP and CBf schemes. The results in this work are obtained by performing the analysis in the large system limit where the dimensions of the system i.e., the numbers of users and transmit antennas tend to infinity with their ratio being fixed. The large system analysis mainly exploits the eigenvalue distribution of large random matrices. For examples, it has been used to derive the asymptotic performance of linear multiuser receivers in CDMA communications in early 2000 (see [27]), single-cell broadcast channels with RCI for various channel conditions [24], [28]–[30], base station cooperations in downlink multi-cell networks (see e.g., [17], [25]). The asymptotic

performance measure becomes a deterministic quantity and can have close-form/compact expressions. Hence, it can be used to derive the optimal parameters for the system design. Moreover, it can provide a good approximation of, hence insights on, the performance of the finite-size (or even small-size) systems.

Similar to [2] and [14], we perform the feedback optimization in interference-coordination scheme (CBf). As in [14], we also investigate the feedback optimization for the analog and digital feedback schemes. However, different from those works, we do not assume the intra-cell TDMA in each cell, and hence each user experiences both intra-cell and inter-cell interference. We also consider a different type of precoder i.e., the RCI. Moreover, we also analyze the feedback optimization for different level of cooperations between the base stations, including the MCP setup, and try to capture how we allocate resources available at the user side as the the interfering channel gain varies.

D. Paper Organization and Notation

The rest of the paper is structured as follows. The system model is described in Section II. It starts with the channel model, and the expressions of the transmit signal, precoder and the corresponding SINR for each MCP and CBf. In the end of the section, the feedback schemes and true channel model in term of the channel estimate at the BSs and the channel uncertainty for the analog and digital feedback are presented. The main results for the noisy analog feedback and digital feedback and for different types of coordination are discussed in Section III and IV, respectively. In each section, we begin by discussing the large system result of the SINR for the MCP and CBf and then followed by deriving the corresponding optimal feedback allocation; optimal (uplink) power for the analog feedback and optimal bit partitioning for the digital feedback. The optimal regularization parameter for the RCI precoder is also derived for both types of feedback and cooperation. The end of each section provides numerical results that depict how the optimal feedback allocation and the SINR of each user behave as the interfering channel gain varies. In Section V, we provide some numerical simulations that compare the performance of the system under the analog feedback and digital feedback. The conclusion are drawn in the Section VI and some of the proofs go to the appendices.

Throughout the paper, the following notations are used. $\mathbb{E}[\cdot]$ denotes the statistical expectation. The almost sure convergence, convergence in probability, and mean-square convergence are denoted by $\xrightarrow{a.s.}$, $\xrightarrow{i.p.}$, $\xrightarrow{L_2}$ respectively. The partial derivative of f with respect to (w.r.t.) x is denoted by $\frac{\partial f}{\partial x}$. The circularly symmetric complex Gaussian (CSCG) vector with mean $\boldsymbol{\mu}$ and covariance matrix $\boldsymbol{\Sigma}$ is denoted by $\mathcal{CN}(\boldsymbol{\mu}, \boldsymbol{\Sigma})$. $|a|$ and $\Re[a]$ denote the magnitude and the real part of the complex variable a , respectively. $\|\cdot\|$ represents the Euclidean norm and $\text{Tr}(\cdot)$ denotes the trace of a matrix. \mathbf{I}_N and $\mathbf{0}_N$ denote an $N \times N$ identity matrix and a $1 \times N$ zero entries vector, respectively. $(\cdot)^T$ and $(\cdot)^H$ refer to the transpose and Hermitian transpose, respectively. The angle between vector \mathbf{x} and \mathbf{y} is denoted by $\angle(\mathbf{x}, \mathbf{y})$. LHS and RHS refer to the left-hand and right-hand side of an equation, respectively.

II. SYSTEM MODEL

We consider a symmetric two-cell broadcast channel, as shown in Figure 1, where each cell has K single antenna users and a base station equipped with N antennas. The channel between user k in cell j and the BS in cell i is denoted by row vector $\mathbf{h}_{k,j,i}$ where $\mathbf{h}_{k,j,j} \sim \mathcal{CN}(\mathbf{0}, \mathbf{I}_N)$ and $\mathbf{h}_{k,j,\bar{j}} \sim \mathcal{CN}(\mathbf{0}, \epsilon \mathbf{I}_N)$, for $j = 1, 2$ and $\bar{j} = \text{mod}(j, 2) + 1$. We refer to the $\mathbf{h}_{k,j,j}$ as direct channels and $\mathbf{h}_{k,j,\bar{j}}$ as cross or “interfering” channels. We find it useful to group these into a single channel vector $\mathbf{h}_{k,j} = [\mathbf{h}_{k,j,1} \ \mathbf{h}_{k,j,2}]$.

We consider an FDD system and assume that the users have perfect knowledge of their downlink channels, $\mathbf{h}_{k,j,j}$ and $\mathbf{h}_{k,j,\bar{j}}$. Each user feeds back the channel information to the direct BS and neighboring BS through the corresponding uplink channels. The BSs estimate or recover these channel states and use them to construct the precoder.

The received signal of user k in cell j can be written as

$$y_{k,j} = \mathbf{h}_{k,j,1} \mathbf{x}_1 + \mathbf{h}_{k,j,2} \mathbf{x}_2 + n_{k,j},$$

where $\mathbf{x}_i \in \mathbb{C}^{N \times 1}$, $i = 1, 2$ is the transmitted data from BS i , and $n_{k,j} \sim \mathcal{CN}(0, \sigma_d^2)$ is the noise at the user’s receiver. The transmitted data \mathbf{x}_i depends on the level of cooperation assumed, and will be described in more details in Sections II-A and II-B: we restrict ourselves to linear precoding schemes, more specifically RCI precoder. We assume each BS’s transmission is subject to a power constraint $\mathbb{E}[\|\mathbf{x}_i\|^2] = P_i$. In the MCP case, we relax this constraint to a sum power constraint so that $\mathbb{E}[\|\mathbf{x}\|^2] = \sum_{i=1}^2 P_i = P_t$. In the analysis, we assume $P_1 = P_2 = P$ and denote $\gamma_d = P/\sigma_d^2$.

As already mentioned, in practical scenarios, perfect CSI is difficult to obtain and the CSI at the BSs is obtained through feedback from the users. We are particularly interested in the channel model where we can express the downlink channel between the user k in cell j and BS i as

$$\mathbf{h}_{k,j,i} = \sqrt{\phi_{k,j,i}} \hat{\mathbf{h}}_{k,j,i} + \tilde{\mathbf{h}}_{k,j,i}, \quad (1)$$

where $\hat{\mathbf{h}}_{k,j,i}$ represents the channel estimate, and $\tilde{\mathbf{h}}_{k,j,i}$ the channel uncertainty or estimation error. The channel estimates are used by the BSs to construct the precoder.

The transmitted signal, precoder and SINR for each user for each cooperation scheme will be presented in the following subsections.

A. MCP

As previously mentioned, in the MCP, both BSs share the channel information and data symbols for all users in the network. Therefore, we may consider the network as a broadcast channel with $2N$ transmit antennas and $2K$ single antenna users. The BSs construct the precoding matrix by using the users’ channel estimates. In this work, we consider the RCI precoding, for which the precoding or beamforming vector for user k in cell j , \mathbf{w}_{kj} , can be

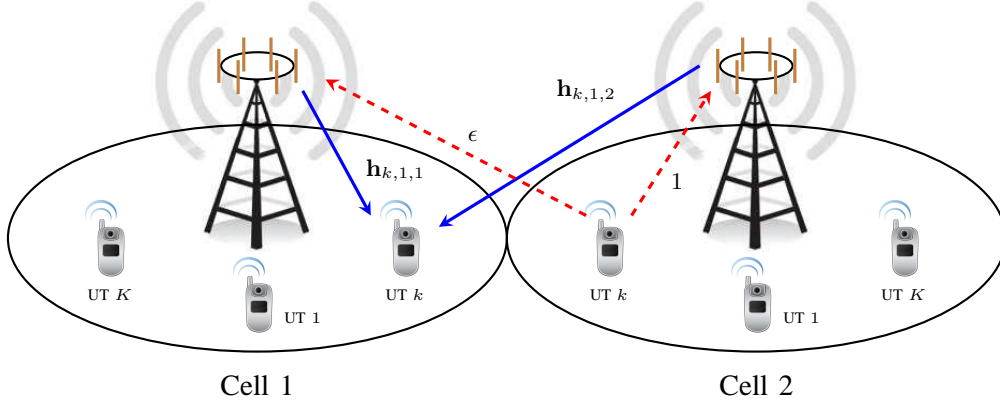


Fig. 1. System model

written as [31]

$$\mathbf{w}_{kj} = c\hat{\mathbf{w}}_{kj} = c \left(\hat{\mathbf{H}}^H \hat{\mathbf{H}} + \alpha \mathbf{I}_{2N} \right)^{-1} \hat{\mathbf{h}}_{k,j}^H,$$

where $\hat{\mathbf{h}}_{k,j} = [\hat{\mathbf{h}}_{k,j,1} \ \hat{\mathbf{h}}_{k,j,2}]$ and $\hat{\mathbf{H}} = [\hat{\mathbf{h}}_{1,1}^H \ \hat{\mathbf{h}}_{2,1}^H \ \cdots \ \hat{\mathbf{h}}_{K,1}^H \ \hat{\mathbf{h}}_{1,2}^H \ \hat{\mathbf{h}}_{2,2}^H \ \cdots \ \hat{\mathbf{h}}_{K,2}^H]^H$. The transmitted data vector can be expressed as

$$\mathbf{x} = c \sum_{j=1}^2 \sum_{k=1}^K \hat{\mathbf{w}}_{kj} s_{kj},$$

where $s_{kj} \sim \mathcal{CN}(0, 1)$ denotes the symbol to be transmitted to user k in cell j . It is also assumed that the data symbols across the users are independent, i.e., $\mathbb{E}[\mathbf{s}\mathbf{s}^H] = \mathbf{I}_{2N}$, with $\mathbf{s} = [\mathbf{s}_1 \ \mathbf{s}_2]^T$ and $\mathbf{s}_j = [s_{1j} \ s_{2j} \ \cdots \ s_{Kj}]^T$. c is a scaling factor ensuring the total power constraint is met with equality:

$$c^2 = \frac{P_t}{\text{Tr} \left(\left(\hat{\mathbf{H}}^H \hat{\mathbf{H}} + \alpha \mathbf{I}_{2N} \right)^{-2} \hat{\mathbf{H}}^H \hat{\mathbf{H}} \right)}.$$

The received signal at user k in cell j can be written as

$$\begin{aligned} y_{kj} &= \mathbf{h}_{k,j} \mathbf{x} + n_{k,j} = c \mathbf{h}_{k,j} \left(\hat{\mathbf{H}}^H \hat{\mathbf{H}} + \alpha \mathbf{I}_{2N} \right)^{-1} \hat{\mathbf{H}}^H \mathbf{s} + n_{k,j} \\ &= c \mathbf{h}_{k,j} \left(\hat{\mathbf{H}}^H \hat{\mathbf{H}} + \alpha \mathbf{I}_{2N} \right)^{-1} \hat{\mathbf{h}}_{k,j}^H s_{k,j} + c \mathbf{h}_{k,j} \left(\hat{\mathbf{H}}^H \hat{\mathbf{H}} + \alpha \mathbf{I}_{2N} \right)^{-1} \hat{\mathbf{H}}_k^H \mathbf{s}_{k,j} + n_{k,j}, \end{aligned}$$

where $\mathbf{h}_{k,j}$ follows the channel model (1) with $\tilde{\mathbf{h}}_{k,j} = [\tilde{\mathbf{h}}_{k,j,1} \ \tilde{\mathbf{h}}_{k,j,2}]$. The term $\hat{\mathbf{H}}_{k,j}$ and $\mathbf{s}_{k,j}$ are obtained from $\hat{\mathbf{H}}$ and \mathbf{s} by removing the row corresponding to user k in cell j respectively. Hence, the SINR for user k in cell j can be expressed as

$$\text{SINR}_{k,j} = \frac{c^2 \left| \mathbf{h}_{k,j} \left(\hat{\mathbf{H}}^H \hat{\mathbf{H}} + \alpha \mathbf{I}_{2N} \right)^{-1} \hat{\mathbf{h}}_{k,j}^H \right|^2}{c^2 \mathbf{h}_{k,j} \left(\hat{\mathbf{H}}^H \hat{\mathbf{H}} + \alpha \mathbf{I}_{2N} \right)^{-1} \hat{\mathbf{H}}_{k,j}^H \hat{\mathbf{H}}_{k,j} \left(\hat{\mathbf{H}}^H \hat{\mathbf{H}} + \alpha \mathbf{I}_{2N} \right)^{-1} \mathbf{h}_{k,j}^H + \sigma_d^2}. \quad (2)$$

B. Coordinated Beamforming

In this scheme, the base stations only share the channel information, so that, for cell j , \mathbf{x}_j can be expressed as

$$\mathbf{x}_j = c_j \sum_{k=1}^K \hat{\mathbf{w}}_{kj} s_{kj},$$

where as in the MCP case $s_{kj} \sim \mathcal{CN}(0, 1)$ denotes the symbol to be transmitted to user k in cell j . The constant c_j is chosen to satisfy the per-BS power constraint, that is, $\mathbb{E}[\|\mathbf{x}_j\|^2] = P_j$. Hence, $c_j^2 = \frac{P_j}{\sum_{k=1}^K \|\hat{\mathbf{w}}_{kj}\|^2}$. We let

$$\hat{\mathbf{w}}_{kj} = \left(\alpha \mathbf{I}_N + \sum_{(l,m) \neq (k,j)} \hat{\mathbf{h}}_{l,m,j}^H \hat{\mathbf{h}}_{l,m,j} \right)^{-1} \hat{\mathbf{h}}_{k,j,j},$$

which is an extension of regularized zero-forcing to the coordinated beamforming setup [17]. Note that designing the precoding matrix at BS j requires *local* CSI only (the $\hat{\mathbf{h}}_{k,i,j}$ from BS j to all users, but not the channels from the other BS to the users). The SINR of user k in cell j can be expressed as

$$\text{SINR}_{k,j} = \frac{c_j^2 |\mathbf{h}_{k,j,j} \mathbf{w}_{kj}|^2}{\sum_{(k',j') \neq (k,j)} c_{j'}^2 |\mathbf{h}_{k,j,j'} \mathbf{w}_{k'j'}|^2 + \sigma_d^2}, \quad (3)$$

where, once again, $\mathbf{h}_{k,j,j}$ and $\mathbf{h}_{k,j,j'}$ follow (1).

C. Analog Feedback through AWGN Channel

In the *analog feedback* scheme, proposed in [15], each user feeds back the CSI to the base stations using the linear analog modulation. Since we skip quantizing and coding the channel information, we can convey this information very rapidly [15]. We also consider a simple uplink channel model, an AWGN channel. A more realistic multiple access (MAC) uplink channel model could be a subject for future investigation. Each user in cell j feeds back its CSI $\mathbf{h}_{k,j}$ orthogonally (in time). Since each user has to transmit $2N$ symbols (its channel coefficients), it needs $2\kappa N$ channel uses to feed back the CSI, where $\kappa \geq 1$. User k in cell j sends

$$\mathbf{h}_{k,j} \mathbf{\Lambda}_j^{\frac{1}{2}}, \quad (4)$$

where $\mathbf{\Lambda}_j$ is a diagonal matrix such that the first N diagonal entries are equal to λ_{j1} and the remaining diagonal entries are equal to λ_{j2} , with $\lambda_{jj} = 2\nu\kappa P_u$, $\lambda_{j\bar{j}} = 2\epsilon^{-1}(1-\nu)\kappa P_u$ and P_u is the user's average transmit power per channel use. Equation (4) satisfies the uplink power constraint $\mathbb{E}[\|\mathbf{h}_{k,j} \mathbf{\Lambda}_j^{\frac{1}{2}}\|^2] = 2\kappa N P_u$. Thus, the power allocated to feedback the direct and interfering channel is controlled by $\nu \in [0, 1]$. We should note that in (4), it is assumed that κ is an integer. If κN is an integer, we can modulate the signal (4) with $2N \times 2\kappa N$ spreading matrix [15], [21] and the analysis presented below still holds.

Now, let b_ℓ , $\ell = 1, 2, \dots, 2N$, be the ℓ th element of $\mathbf{h}_{k,j}$, λ_ℓ be the corresponding element on the diagonal of $\mathbf{\Lambda}$, and $\epsilon_\ell = \mathbb{E}[b_\ell b_\ell^*]$. When this channel coefficient is transmitted, the signal received by the coordinating BSs is

$$\mathbf{y}_\ell = \sqrt{\lambda_\ell} \begin{bmatrix} \mathbf{1}_N \\ \sqrt{\epsilon} \mathbf{1}_N \end{bmatrix} b_\ell + \mathbf{n}_u = \sqrt{\lambda_\ell} \mathbf{p} b_\ell + \mathbf{n}_u,$$

where $\mathbf{n}_u \in \mathbb{C}^{2N \times 1} \sim \mathcal{CN}(\mathbf{0}, \sigma_u^2 \mathbf{I})$ is the noise vector at the coordinating BSs and $\mathbf{1}_N$ is a column vector of length N with all 1 entries. Using the fact that the path-gain from the users in cell j to BS \bar{j} is ϵ , the MMSE estimate of b_ℓ becomes

$$\hat{b}_\ell = \sqrt{\lambda_\ell \epsilon} \mathbf{p}^T [\lambda_\ell \epsilon \mathbf{p} \mathbf{p}^T + \sigma_u^2 \mathbf{I}_{2N}]^{-1} \mathbf{y}_\ell,$$

and its MMSE is $\sigma_{b_\ell}^2 = \epsilon_\ell - \lambda_\ell \epsilon_\ell^2 \mathbf{p}^T [\lambda_\ell \epsilon \mathbf{p} \mathbf{p}^T + \sigma_u^2 \mathbf{I}_{2N}]^{-1} \mathbf{p}$. We should note that $\{\hat{b}_\ell\}$ are mutually independent. By using the property of MMSE estimation, we can express $\mathbf{h}_{k,j,i}$ as

$$\mathbf{h}_{k,j,i} = \hat{\mathbf{h}}_{k,j,i} + \tilde{\mathbf{h}}_{k,j,i}, \quad (5)$$

where $\hat{\mathbf{h}}_{k,j,i}$ represents the channel estimate, and $\tilde{\mathbf{h}}_{k,j,i}$ the channel uncertainty or estimation error. Note that the entries of each vector $\hat{\mathbf{h}}_{k,i,j}$ and $\tilde{\mathbf{h}}_{k,i,j}$ are independent and identically distributed (i.i.d) and distributed according to $\mathcal{CN}(0, \omega_{ji})$ and $\mathcal{CN}(0, \delta_{ji})$, respectively, where

$$\delta_{ji} = \begin{cases} \frac{1}{1+\nu\bar{\gamma}_u}, & j = i \\ \frac{\epsilon}{1+(1-\nu)\bar{\gamma}_u}, & j \neq i, \end{cases}, \quad \omega_{ji} = \begin{cases} \frac{\nu\bar{\gamma}_u}{1+\nu\bar{\gamma}_u}, & j = i \\ \frac{\epsilon(1-\nu)\bar{\gamma}_u}{1+(1-\nu)\bar{\gamma}_u}, & j \neq i, \end{cases} \quad (6)$$

and $\bar{\gamma}_u = 2\gamma_u\kappa(1+\epsilon)$ with $\gamma_u = NP_u/\sigma_u^2$. The channel estimates are used by the BSs to construct the precoder. Since each δ_{ij} and ω_{ij} are identical for all users then we denote $\delta_d = \delta_{jj}, \delta_c = \delta_{j\bar{j}}, \omega_d = \omega_{jj}$ and $\omega_c = \omega_{j\bar{j}}$. From (6), it follows that $\omega_d = 1 - \delta_d$ and $\omega_c = \epsilon - \delta_c$.

D. Quantized Feedback via RVQ

In the digital feedback case, user k in cell j uses $B_{k,j,j}$ and $B_{k,j,\bar{j}}$ bits to quantize or feedback the direct and interfering channels, respectively. The total number of feedback bits is assumed to be fixed. It is also assumed that each user has different codebooks: $\mathcal{U}_{k,j,j}$ with size $2^{B_{k,j,j}}$ and $\mathcal{U}_{k,j,\bar{j}}$ with size $2^{B_{k,j,\bar{j}}}$, to quantize the direct and interfering channel, respectively. Moreover, these codebooks are different for each user. In this work, $B_{k,j,j}$ is the same for all users and $B_{k,j,j} = B_d, \forall k, j = 1, 2$. Similarly, $B_{k,j,\bar{j}} = B_c, \forall k, j = 1, 2$. The total number of feedback bits is denoted by B_t , where $B_t = B_d + B_c$.

Since the optimal codebook design for the quantized feedback is not known yet, therefore in this paper, for analytical tractability, we consider the well known RVQ scheme. As suggested by its name, RVQ uses a random vector quantization codebook where the quantization vectors in the codebook are independently chosen from the isotropic distribution on the N -dimensional unit sphere [16], [20]. The codebook is known by the base station and the user. The user quantizes its channel by finding the quantization vector in the codebook which is closest to its channel vector and feedbacks the index of the quantization vector to the BSs. We should note that only the channel direction is quantized. Most of the works that employ RVQ for the feedback model assume that only

channel direction information is sent to the BSs. As mentioned in [20], the channel norm information can also be used for some problems that need channel quality information (CQI) such as power allocation across the channel and users scheduling [32].

The user k in cell j finds its quantization vector for the channel $\mathbf{h}_{k,j,i}$ according to

$$\hat{\mathbf{u}}_{k,j,i} = \arg \max_{\mathbf{u}_{k,j,i} \in \mathcal{U}_{k,j,i}} \frac{|\mathbf{h}_{k,j,i} \mathbf{u}_{k,j,i}^H|}{\|\mathbf{h}_{k,j,i}\|}.$$

The quantization error or distortion $\tau_{k,j,i}^2$ is defined as

$$\tau_{k,j,i}^2 = 1 - \frac{\|\mathbf{h}_{k,j,i} \hat{\mathbf{u}}_{k,j,i}\|^2}{\|\mathbf{h}_{k,j,i}\|^2} = \sin^2(\angle(\mathbf{h}_{k,j,i}/\|\mathbf{h}_{k,j,i}\|, \hat{\mathbf{u}}_{k,j,i})).$$

It is a random variable whose distribution is equivalent to the minimum of $2^{B_{k,j,i}}$ beta random variables with parameters $N-1$ and 1 (see [20], [33]). Each realization of $\tau_{k,j,i}$ is different for each user even though the users have the same amount of feedback bits.

Having obtained $\hat{\mathbf{u}}_{k,j,i}$, each user then sends its index in the codebook and also the channel magnitude $\|\mathbf{h}_{k,j,i}\|$ (see also [32]). By assuming that the BSs can receive the information perfectly, the channel estimate at the BS can be written as

$$\hat{\mathbf{h}}_{k,j,i} = \|\mathbf{h}_{k,j,i}\| \hat{\mathbf{u}}_{k,j,i}. \quad (7)$$

Note that $\hat{\mathbf{h}}_{k,j,i}$ has the same statistical distribution as $\mathbf{h}_{k,j,i}$ i.e., $\hat{\mathbf{h}}_{k,j,i} \sim \mathcal{CN}(0, \epsilon_{ji} \mathbf{I}_N)$, where $\epsilon_{ji} = 1$ when $i = j$ and otherwise, $\epsilon_{ji} = \epsilon$.

From [20], [34], we can model $\mathbf{h}_{k,j,i}$ as follows

$$\mathbf{h}_{k,j,i} = \sqrt{1 - \tau_{k,j,i}^2} \hat{\mathbf{h}}_{k,j,i} + \tau_{k,j,i} \|\mathbf{h}_{k,j,i}\| \mathbf{z}_{k,j,i}, \quad (8)$$

where $\mathbf{z}_{k,j,i}$ is isotropically distributed in the null-space of $\hat{\mathbf{h}}_{k,j,i}$ and is independent of $\tau_{k,j,i}$. Moreover, $\mathbf{z}_{k,j,i}$ can be rewritten as

$$\mathbf{z}_{k,j,i} = \frac{\mathbf{v}_{k,j,i} \Pi_{\hat{\mathbf{h}}_{k,j,i}}^\perp}{\|\mathbf{v}_{k,j,i} \Pi_{\hat{\mathbf{h}}_{k,j,i}}^\perp\|},$$

where $\Pi_{\hat{\mathbf{h}}_{k,j,i}}$ is the projection matrix in the column space of $\hat{\mathbf{h}}_{k,j,i}$, $\Pi_{\hat{\mathbf{h}}_{k,j,i}}^\perp = \mathbf{I}_N - \frac{\hat{\mathbf{h}}_{k,j,i}^H \hat{\mathbf{h}}_{k,j,i}}{\|\hat{\mathbf{h}}_{k,j,i}\|^2}$ and $\mathbf{v}_{k,j,i} \sim \mathcal{CN}(\mathbf{0}, \mathbf{I}_N)$ is independent of $\hat{\mathbf{h}}_{k,j,i}$. It is clear that the channel model (8) has the same structure as (1) with $\phi_{k,j,i} = 1 - \tau_{k,j,i}^2$ and $\tilde{\mathbf{h}} = \tau_{k,j,i} \|\mathbf{h}_{k,j,i}\| \mathbf{z}_{k,j,i}$.

E. Achievable and limiting sum-rate

Besides $\text{SINR}_{k,j}$, another relevant performance measure is the achievable rate. For the user k at cell j , it is defined as

$$R_{k,j} = \log_2(1 + \text{SINR}_{k,j}), \quad (9)$$

It is obtained by treating the interferences as noise or equivalently performing single-user decoding at the receiver. Observing (9), it is obvious that there is a one-to-one continuous mapping between the SINR and the achievable rate (see also [35]). The total sum-rate, or just the sum-rate, can then be defined as follows

$$R_{\text{sum}} = \sum_{j=1}^2 \sum_{k=1}^K R_{kj}. \quad (10)$$

As shown later in Section III and IV, as $K, N \rightarrow \infty$, we have

$$\text{SINR}_{kj} - \text{SINR}^\infty \rightarrow 0, \quad (11)$$

where SINR^∞ is a deterministic quantity and also called the limiting SINR. It is also shown that the limiting SINR is the same for all users. By using the result (11) and based on the continuous mapping theorem [36], the following

$$\frac{1}{2N} \mathbb{E}[R_{\text{sum}}] - R_{\text{sum}}^\infty \rightarrow 0$$

holds (see also [24]) where the limiting achievable sum-rate can be expressed as $R_{\text{sum}}^\infty = \beta \log_2(1 + \text{SINR}^\infty)$. For the numerical simulations, we also introduce the normalized sum-rate difference, defined as

$$\Delta R_{\text{sum}} = \frac{\frac{1}{2N} \mathbb{E}[R_{\text{sum}}] - R_{\text{sum}}^\infty}{\frac{1}{2N} \mathbb{E}[R_{\text{sum}}]}, \quad (12)$$

that quantifies the sum-rate difference, $\frac{1}{2N} \mathbb{E}[R_{\text{sum}}] - R_{\text{sum}}^\infty$, compared to the (actual) finite-size system average sum-rate.

III. MCP AND CBF WITH NOISY ANALOG FEEDBACK

In this section, we will discuss the large system results and feedback optimization for the MCP and CBF by using the analog feedback model discussed in Section II-C. First, the large system limit expression for the SINR is derived. Then, the corresponding optimal regularization parameter that maximizes the limiting SINR is investigated. Finally, the optimal ν that maximizes the limiting SINR that already incorporates the optimal regularization parameter will be discussed.

A. MCP

We start with the theorem that states the large system limit of the SINR (2).

Theorem 1. *Let $\rho_{MAF} = (\omega_d + \omega_c)^{-1} \alpha / N$ and $g(\beta, \rho)$ be the solution of $g(\beta, \rho) = \left(\rho + \frac{\beta}{1+g(\beta, \rho)} \right)^{-1}$. In the large system limit, the SINR of MCP given in (2) converges in probability to a deterministic quantity given by*

$$\text{SINR}_{MCPAF}^\infty = \gamma_e g(\beta, \rho_{MAF}) \frac{1 + \frac{\rho_{MAF}}{\beta} (1 + g(\beta, \rho_{MAF}))^2}{\gamma_e + (1 + g(\beta, \rho_{MAF}))^2}, \quad (13)$$

where the effective SNR γ_e is expressed as

$$\gamma_e = \frac{\omega_d + \omega_c}{\delta_d + \delta_c + \frac{1}{\gamma_d}} = \frac{1 - \delta_d + \epsilon - \delta_c}{\delta_d + \delta_c + \frac{1}{\gamma_d}}. \quad (14)$$

Proof: See Appendix II-A ■

It is obvious from above that the limiting SINR is the same for all users in both cells. This is due to the channel statistics of all users in both cells are the same. The channel uncertainty, captured by ω_\bullet and δ_\bullet , affects the system performance (limiting SINR) via the effective SNR and regularization parameter $\rho_{M,AF}$.

As discussed previously, the (effective) regularization parameter $\rho_{M,AF}$ controls the amount of interference introduced to the users and provides the trade-off between suppressing the inter-user interference and increasing desired signal energy. The optimal choice of $\rho_{M,AF}$ that maximizes (13) is given in the following.

Corollary 1. *The optimal $\rho_{M,AF}$ that maximizes $SINR_{MCP,AF}^\infty$ is*

$$\rho_{M,AF}^* = \frac{\beta}{\gamma_e}, \quad (15)$$

and the corresponding limiting SINR is

$$SINR_{MCP,AF}^{*,\infty} = g(\beta, \rho_{M,AF}^*). \quad (16)$$

Proof: The proof follows easily from [37]. ■

It is interesting to see that the limiting SINR expression with $\rho_{M,AF}^*$ becomes simpler and it depends only the cell-loading (β) and the effective SNR. Clearly from (14), γ_e is a function of the total MSE, $\delta_t = \delta_d + \delta_c$, that can be thought as a reasonable measure of the CSIT quality. Thus, $\rho_{M,AF}^*$ adjusts its value as δ_t changes. Now, from (14), it is obvious that γ_e is a decreasing function of δ_t . As a result, $\rho_{M,AF}^*$ is increasing with δ_t . In other words, if the total quality of CSIT improves then the regularization parameter becomes smaller. In the perfect CSIT case, i.e., $\delta_t = 0$, and in the high SNR regime, $\rho_{M,AF}^*$ goes to zero and we have the ZF precoder.

Now, we will investigate how to allocate ν to maximize the limiting SINR (16), or equivalently $g(\beta, \rho_{M,AF}^*)$. ν is captured by γ_e (or $\rho_{M,AF}^*$) via δ_d . It can be shown that g is decreasing (increasing) in $\rho_{M,AF}$ (γ_e). Then, for a fixed β the limiting SINR is maximized by solving the following optimization problem

$$\max_{\nu \in [0,1]} \gamma_e = \frac{\epsilon - \delta_c + 1 - \delta_d}{(\delta_d + \delta_c) + \frac{1}{\gamma_d}}.$$

As mentioned earlier, γ_e is a decreasing function of δ_t . Thus, the optimization problem above can be rewritten as

$$\min_{\nu \in [0,1]} \delta_t = \delta_d + \delta_c = \frac{1}{\nu \bar{\gamma}_u + 1} + \frac{\epsilon}{(1 - \nu) \bar{\gamma}_u + 1}. \quad (17)$$

From the above, it is very interesting to note that *the optimal ν that maximizes $SINR_{MCP}^{*,\infty}$ is the same as the one that minimizes the total MSE, δ_t .*

It is easy to check that the optimization problem above is a convex program and the optimal ν , denoted by ν^* ,

can be expressed as follows

$$\nu^* = \begin{cases} 0, & \sqrt{\epsilon} \geq \bar{\gamma}_u + 1 \\ 1, & \sqrt{\epsilon} \leq \frac{1}{\bar{\gamma}_u + 1} \\ \frac{1 + \frac{1}{\bar{\gamma}_u}(1 - \sqrt{\epsilon})}{1 + \sqrt{\epsilon}}, & \text{otherwise.} \end{cases} \quad (18)$$

As a result, for $\sqrt{\epsilon} \leq \frac{1}{\bar{\gamma}_u + 1}$, the BSs should not waste resources trying to learn about the “interfering” channel states. In this situation, *the coordination breaks down* and the base stations perform SCP. The completely opposite scenario, in which the BSs should not learn the “direct” channels, occurs when $\sqrt{\epsilon} \geq \bar{\gamma}_u + 1$. Clearly, this can only happen if $\epsilon > 1$. When $\sqrt{\epsilon} \geq \bar{\gamma}_u + 1$, the BSs also perform SCP but each BS transmits to the users in the neighboring cell.

We end this subsection by characterizing the behavior of γ_e (equivalently $\text{SINR}_{\text{MCP}}^{*,\infty}$), after optimal feedback power allocation, as the cross channel gain ϵ varies. This also implicitly shows how the total MSE, δ_t , affects the limiting SINR. Let $\check{\gamma}_u = \frac{\bar{\gamma}_u}{(1+\epsilon)}$. We analyze the different cases in (18) separately.

1) $\sqrt{\epsilon} \leq \frac{1}{\bar{\gamma}_u + 1}$: This is the case when the BSs perform SCP for the users in their own cell. For fixed $\check{\gamma}_u$, this inequality is equivalent to $\epsilon \leq \epsilon_{\text{max}}^{\text{SCP}}$, where $\epsilon_{\text{max}}^{\text{SCP}} \geq 0$ satisfies $\sqrt{\epsilon_{\text{max}}^{\text{SCP}}} = \frac{1}{\check{\gamma}_u(1+\epsilon_{\text{max}}^{\text{SCP}})+1}$. Now, by taking the first derivative $\frac{\partial \gamma_e}{\partial \epsilon}$ and setting it to zero, the (unique) stationary point is given by

$$\epsilon_{\text{AF}}^{\text{SCP}} = \frac{1}{\sqrt{\gamma_d \check{\gamma}_u}} - 1.$$

If $\sqrt{\epsilon_{\text{AF}}^{\text{SCP}}} \in [0, \sqrt{\epsilon_{\text{max}}^{\text{SCP}}}]$, it is easy to check that the limiting SINR is increasing until $\epsilon = \epsilon_{\text{AF}}^{\text{SCP}}$ and then decreasing. If $\sqrt{\gamma_d \check{\gamma}_u} > 1$ then $\epsilon_{\text{AF}}^{\text{SCP}} < 0$, or equivalently, $\frac{\partial \gamma_e}{\partial \epsilon} < 0$. Consequently, for this case, the limiting SINR is decreasing in ϵ . Moreover, $\sqrt{\epsilon_{\text{AF}}^{\text{SCP}}} \geq \sqrt{\epsilon_{\text{max}}^{\text{SCP}}}$ if the following condition holds

$$\sqrt{\gamma_d \check{\gamma}_u}(2 - 2\gamma_d - \check{\gamma}_u) \geq (2\gamma_d \check{\gamma}_u - \gamma_d - \check{\gamma}_u), \quad (19)$$

in which case $\frac{\partial \gamma_e}{\partial \epsilon} > 0$, which implies that the limiting SINR always increases over ϵ for this case.

This behavior of γ_e as a function of ϵ can be intuitively explained as follows. When $\nu = 1$, the total MSE is $\delta_t = \frac{1}{(1+\epsilon)\check{\gamma}_u+1} + \epsilon$, where the first and second terms are δ_d and δ_c , respectively. As ϵ increases, δ_d decreases whereas δ_c increases. This shows that there is a trade-off between the quality of the direct channel and the strength of the interference. The trade-off is also influenced by parameters γ_d and $\check{\gamma}_u$. As shown in the analysis, when $\sqrt{\gamma_d \check{\gamma}_u} > 1$, the effect of cross channel to the limiting SINR dominates. In contrast, if the condition in (19) is satisfied, the effect of the quality of the direct channel (δ_t) becomes dominant. If the aforementioned conditions do not hold, δ_t causes the SINR to increase until $\epsilon_{\text{AF}}^{\text{SCP}}$ and after that the interference from the cross channel takes over as the dominant factor, thereby reducing the limiting SINR.

2) $\bar{\gamma}_u + 1 \geq \sqrt{\epsilon} \geq \frac{1}{\bar{\gamma}_u + 1}$: Here, the BSs perform MCP. By taking $\frac{\partial \gamma_e}{\partial \epsilon}$ in that interval of ϵ , it can be shown that we have a unique stationary which we denote as $\sqrt{\epsilon_{\text{AF}}^{\text{M}}}$. We can also show that γ_e is a convex function for $\epsilon \in [0, 1]$ and

is increasing for $\epsilon \geq 1$. Thus, if $\frac{1}{\bar{\gamma}_u + 1} \leq \sqrt{\epsilon_{AF}^M} \leq \bar{\gamma}_u + 1$, the limiting SINR will decrease for $\sqrt{\epsilon} \in [\frac{1}{\bar{\gamma}_u(1+\epsilon)+1}, \sqrt{\epsilon_{AF}^M}]$ and increase after that; Otherwise, the limiting SINR increases in the region. Here, for $\sqrt{\epsilon} \in [\frac{1}{\bar{\gamma}_u + 1}, 1]$, we still can see the effect of the trade-off within δ_t to the limiting SINR as ϵ changes. In that interval, the quality of the direct channel becomes better as ϵ increases; However, that of the cross channel decreases and this affects the SINR badly until ϵ_{AF}^M . After this point, the improvement in the quality of the direct channel will outweigh the deterioration of that of the cross channel, causing the SINR to increase.

3) $\sqrt{\epsilon} \geq \bar{\gamma}_u + 1$: In this case, each BS performs SCP, but serves the other cell's users. We can establish that $\frac{\partial \gamma_e}{\partial \epsilon} > 0$. Hence, for this case, the limiting SINR is increasing in ϵ .

B. Coordinated Beamforming

Theorem 2. Let $\rho_{CAF} = \frac{\alpha}{N}$, and let Γ_A be the solution of the following cubic equation

$$\Gamma_A = \frac{1}{\rho_{CAF} + \frac{\beta\omega_c}{1+\omega_c\Gamma_A} + \frac{\beta\omega_d}{1+\omega_d\Gamma_A}}. \quad (20)$$

In the large system limit, the SINR of the coordinated beamforming given in (3) converges almost surely to a deterministic quantity given by

$$SINR_{CBf,AF}^\infty = \frac{\frac{\omega_d}{\beta}\Gamma_A \left[\rho_{CAF} + \frac{\beta\omega_c}{(1+\omega_c\Gamma_A)^2} + \frac{\beta\omega_d}{(1+\omega_d\Gamma_A)^2} \right]}{\left(\frac{1}{\gamma_d} + \delta_d + \delta_c + \frac{\omega_d}{(1+\omega_d\Gamma_A)^2} + \frac{\omega_c}{(1+\omega_c\Gamma_A)^2} \right)}. \quad (21)$$

Proof: See Appendix III-A ■

Similar to the MCP case, the limiting SINR expression (21) is the same for all users. By comparing (15) and (22), it is also interesting to see that $\rho_{CAF} = \rho_{MAF}$ for a given α . The optimal ρ_{CAF} that maximizes the limiting SINR (21) is given in the following.

Corollary 2. The limiting SINR (21) is maximized by choosing the regularization parameter according to

$$\rho_{CAF}^* = \beta \left(\frac{1}{\gamma_d} + \delta_d + \delta_c \right). \quad (22)$$

and the corresponding limiting SINR is

$$SINR_{CBf,AF}^{*,\infty} = \omega_d \Gamma_A^*, \quad (23)$$

where Γ_A^* is Γ_A with $\rho_{CAF} = \rho_{CAF}^*$.

Proof: Let $\gamma_{eff} = \beta (\gamma_d^{-1} + \delta_d + \delta_c)$ and $\Psi = \frac{\beta\omega_d}{(1+\omega_d\Gamma_A)^2} + \frac{\beta\omega_c}{(1+\omega_c\Gamma_A)^2}$. It is easy to show that

$$\frac{\partial SINR_{CBf,AF}^\infty}{\partial \rho_{CAF}} = \omega_d \frac{\gamma_{eff} - \rho_{CAF}}{[\gamma_{eff} + \Psi]^2} \frac{\partial \Psi}{\partial \rho_{CAF}}, \quad (24)$$

where $\frac{\partial \Psi}{\partial \rho_{CAF}} = -2\beta \frac{\partial \Gamma_A}{\partial \rho_{CAF}} \left(\frac{\omega_d^2}{(1+\omega_d\Gamma_A)^3} + \frac{\omega_c^2}{(1+\omega_c\Gamma_A)^3} \right) > 0$ with $\frac{\partial \Gamma_A}{\partial \rho_{CAF}} < 0$ is given by (61). Thus, it follows that $\rho_{CAF}^* = \gamma_{eff}$ is the unique stationary point and the global optimizer. Plugging back ρ_{CAF} into (21) yields (23). ■

Similar to the MCP case, the corollary above shows that the optimal regularization parameter adapts to the changes of CSIT quality and it is a decreasing function of δ_t .

Finding ν that maximizes the limiting SINR of the CBf is more complicated than in the MCP case. It is equivalent to maximizing $\omega_d \Gamma$, such that $\nu \in [0, 1]$: this is a non-convex program. However, the maximizer ν^* is one of followings: the boundaries of the feasible set ($\nu = \{0, 1\}$) or the stationary point, denoted by ν° , which is the solution of

$$\nu^\circ = -\frac{\Gamma_A^*}{\frac{\partial \Gamma_A^*}{\partial \rho_{C,AF}^*}(1 + \nu^\circ \bar{\gamma}_u)}. \quad (25)$$

The point $\nu = 0$ can be eliminated from the feasible set since the derivative of the limiting SINR with respect to ν at this point is always positive.

C. Numerical Results

Since propagation channels fluctuate, the SINR expressions in (2) and (3) are random quantities. Consequently, the average sum-rates are also random. Figure 2 illustrates how the random average sum-rates approach the limiting sum-rates as the dimensions of the system increase. This is quantified by the normalized sum-rate difference which is defined in (12). The average sum-rate is obtained by averaging the sum-rates over 1000 channel realizations. The optimal regularization parameter and power splitting obtained in the large system analysis are used in computing the limiting and average sum-rates. We can see that as the system size increases, the normalized sum-rate difference becomes smaller and this hints that the approximation of the average sum-rate by the limiting sum-rate becomes more accurate. The difference is already about 1.3% and 0.5% for the MCP and CBf respectively for $N = 60, K = 36$.

Figure 3 describes the applicability of the large system results into finite-size systems. We choose a reasonable system-size in practice, i.e., $N = 10, K = 6$. Then, 250 channel realizations are generated. For each channel realization, with a fixed regularization parameter of the precoder, the optimal ν , denoted by ν_{FS}^* , is computed. Then the resulting average sum-rate is compared to the average sum-rate that using ν^* from the large system analysis, i.e., (18) and (25), for different values of ϵ . We can see that the normalized average sum-rate difference, i.e., $\frac{\mathbb{E}[|R_{\text{sum}}(\nu_{FS}) - R_{\text{sum}}(\nu^*)|]}{R_{\text{sum}}(\nu_{FS})}$, for CBf has a peak around 4% that can be considered as a reasonable value for the chosen system size. For MCP, it is less than 0.47%. To this end, our simulation results indicate that the large system results discussed earlier approximate the finite-system quite well.

In the following, we present some numerical simulations that visualize the characteristics of the optimal ν^* (in the large system limit) and the corresponding limiting SINR for each cooperation scheme. We are primarily interested in their characteristics when the interfering channel gain ϵ varies, as depicted in Figure 4. In general, we can see that for the same system parameters, the CBf scheme allocates more power to feed back the direct channel compared to the MCP. From Figure 4(a), we can see that for values of ϵ ranging from 0 up to a certain threshold (denoted by $\epsilon_M^{\text{th}} = \epsilon_{\text{max}}^{\text{SCP}}$ and ϵ_C^{th} for MCP and CBf respectively), the optimal ν is 1: in other words, it is optimal in

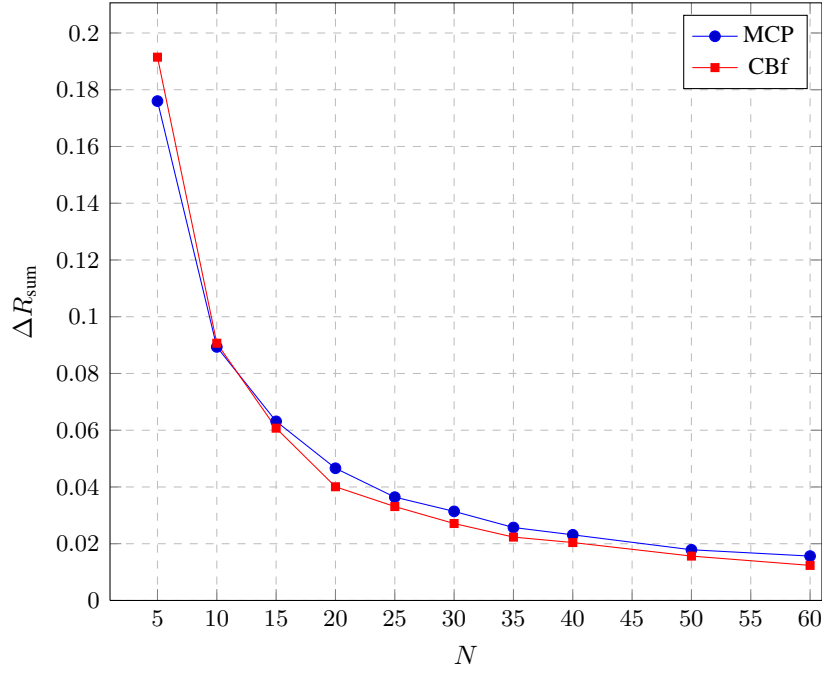


Fig. 2. The normalized sum-rate difference for different system dimensions with $\beta = 0.6$, $\epsilon = 0.5$, $\gamma_d = 10$ dB and $\gamma_u = 0$ dB.

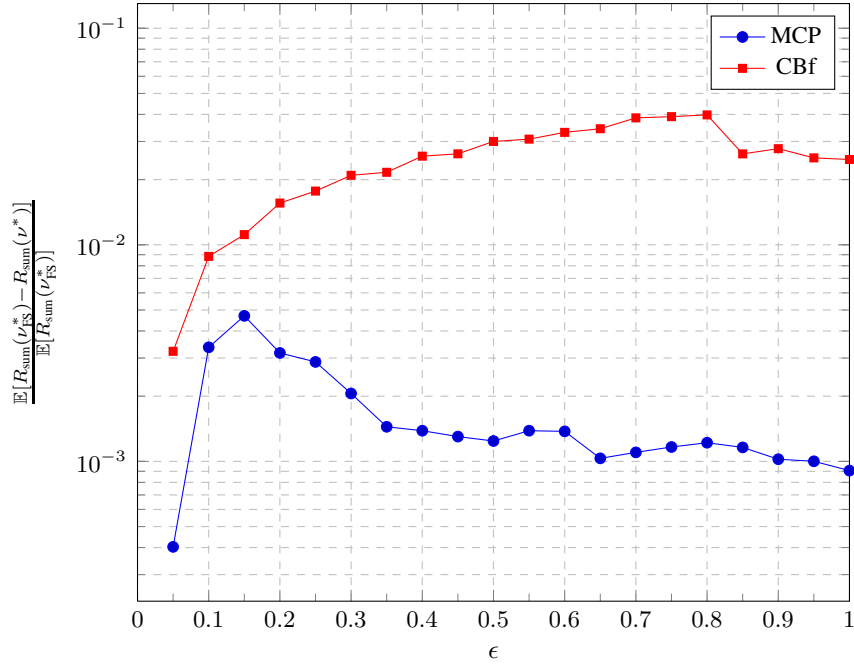


Fig. 3. The normalized average sum-rate difference of the finite-size system by using the ν_{FS} and ν^* with $N = 10$, $\beta = 0.6$, $\gamma_d = 10$ dB and $\gamma_u = 0$ dB.

this range for the BSs not to try to get information about the cross channels and to construct the precoder based on the direct channel information only. Effectively, the two schemes reduce to the SCP scheme when $\nu^* = 1$: as a result, the same limiting SINR is achieved by both schemes.

In Figure 4(b), we can observe a peculiar behavior of the limiting SINR of MCP, which we already highlighted

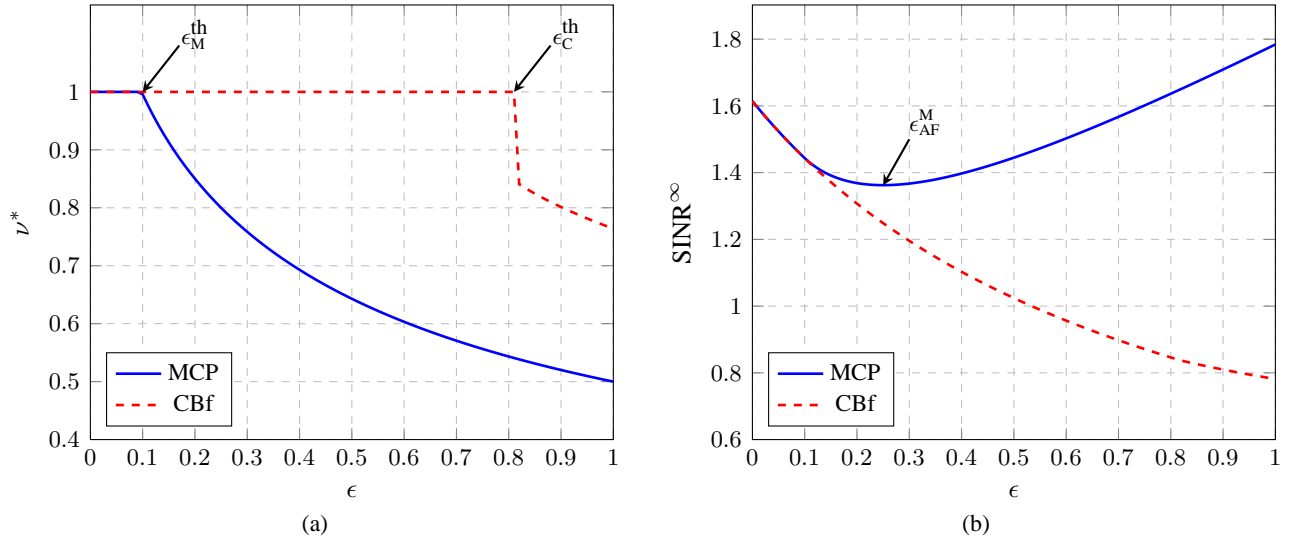


Fig. 4. (a) The optimal ν^* and (b) the limiting SINR for the MCP and CBf scheme as ϵ varies in $[0, 1]$ with $\beta = 0.6$, $\gamma_d = 10$ dB, $\gamma_u = 0$ dB.

in the analysis of Section III-A. When $\sqrt{\epsilon} \leq \frac{1}{\gamma_u + 1}$, i.e. when $\nu^* = 1$, the SINR is decreasing as ϵ increases. After that the SINR is still decreasing until ϵ reaches ϵ_{AF}^M and then increasing: this reflects the trade-off between δ_c and δ_d . Note that this initial decrease does not occur in the perfect CSI case where the SINR is strictly increasing in ϵ for MCP. Similar to the MCP case, we can see that the limiting SINR of CBf is decreasing in ϵ when $\nu^* = 1$ (SCP). Moreover, it is still decreasing when both BSs perform CBf.

IV. QUANTIZED FEEDBACK VIA RANDOM VECTOR QUANTIZATION (RVQ)

In this section, we will derive the approximations of the SINR for the MCP (2) and CBf (3) by analyzing them in the large system limit. We use these approximations to optimize the feedback bit allocation, and regularization parameter. This joint optimization problem can be split into two steps. First, we derive the optimal bit allocation, i.e., the optimal $\bar{B}_d = \frac{B_d}{N}$ and $\bar{B}_c = \frac{B_c}{N}$. Plugging the optimal bit allocation back into the limiting SINR expression, we can then proceed to the second step where we obtain the optimal regularization parameter. At the end of the section, some comparisons of the limiting SINR and bit allocation values for the two schemes are illustrated.

A. MCP

Theorem 3. Let $\rho_{M,Q} = (1 + \epsilon)^{-1}\alpha/N$ and $g(\beta, \rho)$ be the solution of $g(\beta, \rho) = \left(\rho + \frac{\beta}{1+g(\beta, \rho)}\right)^{-1}$. In the large system limit, the SINR converges in probability to a deterministic quantity given by

$$SINR_{MCP,Q}^\infty = \gamma_e g(\beta, \rho_{M,Q}) \frac{1 + \frac{\rho_{M,Q}}{\beta} (1 + g(\beta, \rho_{M,Q}))^2}{\gamma_e + (1 + g(\beta, \rho_{M,Q}))^2}, \quad (26)$$

where

$$\gamma_e = \frac{d^2}{1 - d^2 + \frac{1}{\gamma_d(1+\epsilon)}} \quad (27)$$

is defined as the effective SNR and

$$d = \frac{\sqrt{1 - 2^{-\bar{B}_d}} + \epsilon \sqrt{1 - 2^{-\bar{B}_c}}}{1 + \epsilon}. \quad (28)$$

Proof: Refer to Appendix II-B. ■

Theorem 3 shows that the limiting SINR is the same for all users in both cells. This is not surprising given the symmetry in their channel statistics and feedback mechanisms. Moreover, the only dependence of the limiting SINR on the bit allocation is via γ_e , which itself is a function of d : d can be interpreted as a measure of the total quality of the channel estimates; In fact, given that \bar{B}_d and \bar{B}_c are constrained to sum up to \bar{B}_t , d in (28) highlights a trade-off between increasing feedback bits for direct channel and cross channel. Comparing (13) and (26), we can immediately recognize an identical structure between them. The effective SNR expressions (14) and (27) also share a similar construction, where $(1 + \epsilon)d^2$ in (28) can be thought to be equivalent to $\omega_d + \omega_c$.

Now, we move to the first step of the joint optimization i.e., determining the optimal bit allocation that maximizes (26). It is clear from (26) that \bar{B}_d and \bar{B}_c contributes to the limiting SINR through d . It is easy to check that the limiting SINR is an increasing and a convex function of d . Thus, maximizing $\text{SINR}_{\text{MCP,Q}}^\infty$ is equivalent to maximizing d , i.e. solving (cf. Eq. (28)).

$$\max_{x_d \in [X_t, 1]} \sqrt{1 - x_d} + \epsilon \sqrt{1 - \frac{X_t}{x_d}}. \quad (29)$$

where $X_t = 2^{-\bar{B}_t}$, $\bar{B}_t = \frac{B_t}{N}$ and $x_d = 2^{-\bar{B}_d}$. The solution of (29) is presented in the following theorem.

Theorem 4. $\text{SINR}_{\text{MCP,Q}}^\infty$ is maximized by allocating $\bar{B}_d = -\log_2(x_d^*)$ bits to feed back the direct channel information, and $\bar{B}_c = \bar{B}_t - \bar{B}_d$ to feed back the interfering channel information, where x_d^* is the positive (real) solution of the following quartic equation

$$x_d^4 - X_t x_d^3 + (\epsilon X_t)^2 (x_d - 1) = 0. \quad (30)$$

Proof: The first derivative of the objective function over x_d is given by

$$(1 + \epsilon) \frac{\partial \mathbb{E}[d]}{\partial x_d} = \frac{1}{2} \left(-\frac{1}{\sqrt{1 - x_d}} + \frac{1}{x_d^2} \frac{\epsilon X_t}{\sqrt{1 - \frac{X_t}{x_d}}} \right) \quad (31)$$

and $\lim_{x_d \rightarrow X_t} \frac{\partial \mathbb{E}[d]}{\partial x_d} = \infty$, $\lim_{x_d \rightarrow 1} \frac{\partial \mathbb{E}[d]}{\partial x_d} = -\infty$. Moreover, the objective function is a concave function in x_d since

$$(1 + \epsilon) \frac{\partial^2 \mathbb{E}[d]}{\partial x_d^2} = \frac{1}{2} \left(-\frac{1}{2} (1 - x_d)^{-3/2} - \frac{2}{x_d^3} \frac{\epsilon X_t}{\sqrt{1 - \frac{X_t}{x_d}}} - \frac{1}{2} \frac{\epsilon X_t}{x_d^4} \left(1 - \frac{X_t}{x_d} \right)^{-3/2} \right) < 0, \quad x_d \in [X_t, 1].$$

The stationary point, x_d^* , is obtained by setting the derivative equal to 0 and it is the non-negative solution of

$$x_d^4 - X_t x_d^3 + (\epsilon X_t)^2 (x_d - 1) = 0.$$

Since the objective function is concave over x_d , then x_d^* gives the global optimum point. ■

Now, let us discuss how the optimal bit allocation vary with ϵ . Since $x_d = x_d^*$ satisfies (30), then by taking the (implicit) derivative of (30) w.r.t. ϵ , we have

$$\frac{\partial x_d^*}{\partial \epsilon} = \frac{2\epsilon X_t^2(1-x_d)}{4x_d^3 - 3X_t x_d^2 + (\epsilon X_t)^2} > 0, \quad \text{for } X_t \leq x_d^* \leq 1.$$

This implies that as ϵ increases, x_d^* (\bar{B}_d^*) increases (decreases). This is consistent with the intuition that for higher ϵ , more resources would be allocated to quantize the cross channel information. At one of the extremes, i.e., $\epsilon = 0$, $x_d^* = X_t$, or $\bar{B}_d = \bar{B}_t$. If $\epsilon = 0$, $x_d^* = X_t$, so that when there is no interference from the neighboring BS, all feedback bits are used to convey the direct channel states, as expected. At the other extreme, when $\epsilon \rightarrow \infty$, $x_d^* \rightarrow 1$ or $\bar{B}_d \rightarrow 0$. This can be shown by setting the derivative (31) equal to zero and we have

$$\frac{1}{\epsilon} = \frac{X_t \sqrt{1-x_d}}{x_d^2 \sqrt{1-\frac{X_t}{x_d}}}.$$

As $\epsilon \rightarrow \infty$, the left hand side goes to zero and the stationarity is achieved by setting $x_d = 1$.

It is also interesting to see how d , after optimal bit allocation, behaves as the cross channel gain varies. Let d^* is d evaluated at $x_d = x_d^*$. By taking $\frac{\partial d^*}{\partial \epsilon}$, we can show the following property.

Proposition 1. *For $\epsilon \leq 1$, d^* is decreasing in ϵ and increasing for $\epsilon \geq 1$. Consequently, d^* is minimum at $\epsilon = 1$.*

As mentioned previously, x_d^* increases and consequently $1 - x_d^*$ decreases as ϵ increases. On the other side, $\epsilon \sqrt{1 - X_t/x_d^*}$ is getting larger. So, from the calculation we can conclude that d^* is mostly affected by $\sqrt{1 - x_d^*}$ for $\epsilon \leq 1$, while for the other values of ϵ , the other term takes over.

We now proceed to find the optimal $\rho_{M,Q}$ that maximizes $\text{SINR}_{\text{MCP},Q}^\infty$. The result is summarized below.

Theorem 5. *Let γ_e^* be γ_e evaluated at $d = d^*$. The optimal ρ_M that maximizes $\text{SINR}_{\text{MCP}}^\infty(d^*)$ is*

$$\rho_{M,Q}^* = \frac{\beta}{\gamma_e^*}. \quad (32)$$

The corresponding limiting SINR is given by

$$\text{SINR}_{\text{MCP}}^{*,\infty} = g(\beta, \rho_{M,Q}^*).$$

Proof: The equation (26) has the same structure as (13) and thus, (32) follows. ■

From Theorem 5, d^* affects the regularization parameter and the limiting SINR via effective SNR γ_e^* . The latter grows with d^* (cf. (27)). Thus, $\rho_{M,Q}^*$ declines as the CSIT quality, d^* , increases and this behavior is also observed for the cooperation schemes with the analog feedback.

In Proposition 1, we established how d^* changes with ϵ . We can show that γ_e^* has a similar behavior but reaches its minimum at a different value of ϵ due to the last term in the denominator in (27). For $\text{SINR}_{\text{MCP}}^{*,\infty}$, it attains its minimum at $\epsilon = \epsilon_Q^M$, as described in the next proposition.

Proposition 2. Suppose that $\epsilon = \epsilon_Q^M$ satisfies

$$(x_d^*)^2 = \frac{\gamma_d(1 + \epsilon) - \frac{1}{2}}{\epsilon X_t [\gamma_d(1 + \epsilon) + 1 + \frac{\epsilon}{2}]}. \quad (33)$$

Then, $\text{SINR}_{\text{MCP},Q}^{*,\infty}$ decreasing for $\epsilon \leq \epsilon_Q^M$ and increasing for $\epsilon \geq \epsilon_Q^M$.

The characterization of $\text{SINR}_{\text{MCP},Q}^{*,\infty}$ above reminds us a similar behavior of $\text{SINR}_{\text{MCP},\text{AF}}^{*,\infty}$ after optimal power allocation. We can conclude that *the limiting SINR of MCP under both feedback schemes has a common behavior as ϵ varies.*

B. Coordinated Beamforming

Theorem 6. Let $\rho_{c,Q} = \alpha/N$ and Γ_Q be the solution of the following cubic equation

$$\Gamma_Q = \frac{1}{\rho_{c,Q} + \frac{\beta}{1+\Gamma_Q} + \frac{\beta\epsilon}{1+\epsilon\Gamma_Q}}. \quad (34)$$

Let $\phi_d = 1 - 2^{-\bar{B}_d}$, $\phi_c = 1 - 2^{-\bar{B}_c}$, $\delta_d = 2^{-\bar{B}_d}$ and $\delta_c = \epsilon 2^{-\bar{B}_c}$. In the large system limit, the SINR (3) for the quantized feedback via RVQ converges weakly to a deterministic quantity given by

$$\text{SINR}_{\text{CBf},Q}^\infty = - \frac{\phi_d \Gamma_Q^2}{\beta \left(\frac{1}{\gamma_d} + \frac{\phi_d}{(1+\Gamma_Q)^2} + \frac{\phi_c \epsilon}{(1+\epsilon\Gamma_Q)^2} + \delta_d + \delta_c \right) \frac{\partial \Gamma_Q}{\partial \rho}} \quad (35)$$

where

$$-\frac{\partial \Gamma_Q}{\partial \rho_{c,Q}} = \frac{\Gamma_Q}{\rho_{c,Q} + \frac{\beta\epsilon}{(1+\epsilon\Gamma_Q)^2} + \frac{\beta}{(1+\Gamma_Q)^2}}.$$

Proof: See Appendix III-B ■

As in Theorem 3, Theorem 6 shows that the limiting SINR is the same for all users. The quantization error variance of estimating the direct channel, δ_d , affects both the signal strength (via ϕ_d) and the interference energy, in which it captures the effect of the *intra-cell* interference. δ_c , on the other hand, only contributes to the interference term: It represents the quality of the cross channel and determines the strength of the *inter-cell* interference. Since \bar{B}_t is fixed, increasing \bar{B}_d , or equivalently reducing \bar{B}_c , will strengthen the desired signal and reduce the intra-cell interference: it does so, however, at the expense of strengthening the inter-cell interference. Thus, feedback bits' allocation is important in order to improve the performance of the system.

To solve the joint optimization problem, it is useful to write (35) as follows

$$\text{SINR}_{\text{CBf},Q}^\infty = G_1 \frac{1 - x_d}{\frac{1}{\gamma_d} + (1 - x_d)(G_2 - 1) + \epsilon \left(1 - \frac{X_t}{x_d} \right) (G_3 - 1) + 1 + \epsilon},$$

where x_d and X_t are defined as in the previous subsection and for brevity, we denote: $G_1 = -\Gamma_Q^2 \left(\beta \frac{\partial \Gamma_Q}{\partial \rho_{c,Q}} \right)^{-1}$, $G_2 = (1 + \Gamma_Q)^{-2}$ and $G_3 = (1 + \epsilon\Gamma_Q)^{-2}$. The optimal bit allocation can be found by solving the following optimization

problem.

$$\max_{x_d \in [X_t, 1]} \text{SINR}_{\text{CBf}, Q}^{\infty}. \quad (36)$$

The solution of (36) is summarized in the following theorem.

Theorem 7. For a fixed \bar{B}_t , the optimal bit allocation, in term of $x_d = 2^{-\bar{B}_d}$, that maximizes $\text{SINR}_{\text{CBf}, Q}^{\infty}$ is given by

$$x_d^* = \begin{cases} X_t, & \epsilon \leq \frac{X_t(\frac{1}{\gamma_d} + 1)}{1 - G_3 - X_t(2 - G_3)} = \epsilon_{th} \\ X_d = \frac{\epsilon X_t(G_3 - 1) + \sqrt{\epsilon^2 X_t^2 (G_3 - 1)^2 - \epsilon X_t(\frac{1}{\gamma_d} + 1 + \epsilon G_3)(G_3 - 1)}}{\frac{1}{\gamma_d} + 1 + \epsilon G_3}, & \text{otherwise.} \end{cases} \quad (37)$$

Proof: Differentiating the objective function (36), we get

$$\frac{\partial \text{SINR}_{\text{CBf}, Q}^{\infty}}{\partial x_d} = G_1 \frac{-x_d^2(\frac{1}{\gamma_d} + 1 + \epsilon G_3) + \epsilon(G_3 - 1)(2X_t x_d - X_t)}{x_d^2 \left(\frac{1}{\gamma_d} + (1 - x_d)(G_2 - 1) + \epsilon \left(1 - \frac{X_t}{x_d} \right) (G_3 - 1) + 1 + \epsilon \right)^2}$$

and the stationary is given by

$$x_d^{\circ} = \frac{\epsilon X_t(G_3 - 1) + \sqrt{\epsilon^2 X_t^2 (G_3 - 1)^2 - \epsilon X_t(\frac{1}{\gamma_d} + 1 + \epsilon G_3)(G_3 - 1)}}{\frac{1}{\gamma_d} + 1 + \epsilon G_3}. \quad (38)$$

Now let us consider the term $Z = -x_d^2(\frac{1}{\gamma_d} + 1 + \epsilon G_3) + \epsilon(G_3 - 1)(2X_t x_d - X_t)$ in the numerator. It can be verified that the sign of Z is the same as the sign of $\frac{\partial \text{SINR}_{\text{CBf}, Q}^{\infty}}{\partial x_d}$. Thus, $X_d = x_d^{\circ}$ will be the unique positive solution of the quadratic equation $Z = 0$.

It can be also checked that $\frac{\partial Z}{\partial x_d} = -2x_d(\frac{1}{\gamma_d} + 1 + \epsilon G_3) + \epsilon(G_3 - 1)(2X_t) < 0$ and thus, Z is decreasing in x_d . Since at $x_d = 1$, $Z < 0$, we should never allocate $x_d^* = 1$. We will allocate $x_d = X_t$ if $Z \leq 0$ at $x_d = X_t$ (this condition is satisfied whenever $\epsilon \leq \epsilon_{th}$). ■

Unlike the MCP case where $x_d^* = X_t$ only when $\epsilon = 0$, in the CBf, it is optimal for a user to allocate all B_t to the direct channel when $0 \leq \epsilon \leq \epsilon_{th}$. Note that $x_d^* = X_t$ does not imply that the cooperation breaks down or that both BSs perform single-cell processing. It is easy to check that ϵ_{th} increases when \bar{B}_t or γ_d is decreased. This suggests that when the resource for the feedback bits is scarce or the received SNR is low then it is preferable for the user to allocate all the feedback bits to quantize the direct channel. So, in this situation, quantizing the cross channel does more harm to the performance the system. However, as ϵ increases beyond ϵ_{th} , quantizing the cross channel will improve the SINR. We can show that x_d^* , particularly X_d , is increasing in ϵ . In doing that, we need to take the derivative of X_d over ϵ . It is easy to show that Γ_Q is decreasing in ϵ . Then, it follows that G_3 is decreasing in ϵ . Using this fact, we can then show $\frac{\partial X_d}{\partial \epsilon} > 0$. So, as in the case of MCP, this suggests that more resources are allocated to feedback the cross-channel when ϵ increases.

Once we have the optimal bit allocation, we can find the optimal $\rho_{C, Q}$, as we did for the MCP. For that purpose,

we can rewrite (37) w.r.t $\rho_{C,Q}$ as follows

$$x_d^* = \begin{cases} X_t, & \rho_{C,Q} \geq \rho_{th} \\ X_d, & \text{otherwise.} \end{cases}$$

where for given X_t, ϵ and γ_d , the threshold ρ_{th} satisfies $\epsilon = \epsilon_{th}$. So, we have $\text{SINR}_{CBf,Q}^\infty(X_d)$ for $\rho_{C,Q} < \rho_{th}$ and $\text{SINR}_{CBf,Q}^\infty(X_t)$ for other values of $\rho_{C,Q}$.

Now, let us investigate the optimal $\rho_{C,Q}$ when $x_d^* = X_d$. By evaluating $\frac{\partial \text{SINR}_{CBf,Q}^\infty(X_d)}{\partial \rho_{C,Q}} = 0$, we can determine the stationary point, which is given by

$$\rho_{X_d}^\circ = \left\{ (1 - X_d) \left((G'_2 + \epsilon G'_3) \left[\frac{1}{\gamma_d} + X_d + \epsilon \frac{X_t}{X_d} \right] + \epsilon (G_2 G'_3 - G_3 G'_2) \left[-X_d + \frac{X_t}{X_d} \right] \right) - X'_d (G_2 + \epsilon G_3) \gamma_e \right\} \\ \times \frac{\beta}{X'_d \gamma_e + (1 - X_d) \left((1 - X_d) G'_2 + \epsilon \left(1 - \frac{X_t}{X_d} \right) G'_3 \right)},$$

where $\gamma_e = \frac{1}{\gamma_d} + 1 + \epsilon + \epsilon(G_3 - 1) \left(1 - \frac{2X_t}{X_d} + \frac{X_t}{X_d^2} \right)$ and $G'_2 = \frac{\partial G_2}{\partial \rho_{C,Q}}$ and $G'_3 = \frac{\partial G_3}{\partial \rho_{C,Q}}$.

We can show that the derivative is positive for $\rho_{C,Q} \in [0, \rho_{X_d}^\circ)$ and negative for $\rho_{C,Q} \in (\rho_{X_d}^\circ, \infty)$. Since $\text{SINR}_{CBf,Q}^\infty(X_d)$ is defined for $\rho_{C,Q} \leq \rho_{th}$, if $\rho_{X_d}^\circ < \rho_{th}$ then $\text{SINR}_{CBf,Q}^\infty(X_d)$ is increasing for $\rho_{C,Q} \in [0, \rho_{X_d}^\circ]$ and decreasing for $\rho_{C,Q} \in [\rho_{X_d}^\circ, \rho_{th})$. If $\rho_{X_d}^\circ \geq \rho_{th}$ then $\text{SINR}_{CBf,Q}^\infty(X_d)$ is increasing for $\rho_{C,Q} \in [0, \rho_{th})$.

Then, we move to the case when $x_d^* = X_t$. By setting $\frac{\partial \text{SINR}_{CBf,Q}^\infty(X_t)}{\partial \rho_{C,Q}} = 0$, the stationary point is then given by

$$\rho_{X_t}^\circ = \beta \frac{(G'_2 + \epsilon G'_3)(X_t + 1/\gamma_d + \epsilon) + \epsilon(1 - X_t)(G_2 G'_3 - G_3 G'_2)}{(1 - X_t) G'_2}.$$

We can also show that the derivative is positive for $\rho_{C,Q} \in [0, \rho_{X_t}^\circ)$ and negative for $\rho_{C,Q} \in (\rho_{X_t}^\circ, \infty)$. Since $\text{SINR}_{CBf,Q}^\infty(X_t)$ is defined for $\rho_{C,Q} \geq \rho_{th}$, if $\rho_{X_t}^\circ > \rho_{th}$ then $\text{SINR}_{CBf,Q}^\infty(X_t)$ is increasing for $\rho_{C,Q} \in [\rho_{th}, \rho_{X_t}^\circ]$ and decreasing for $\rho_{C,Q} \in [\rho_{X_t}^\circ, \infty)$. If $\rho_{X_t}^\circ \leq \rho_{th}$ then $\text{SINR}_{CBf,Q}^\infty(X_t)$ is decreasing for $\rho_{C,Q} \in [\rho_{th}, \infty)$.

In what follows, by knowing the stationary point in both regions of ρ , we will investigate how to obtain the optimal $\rho_{C,Q}$, denoted by $\rho_{C,Q}^*$, for $\rho_{C,Q} \in [0, \infty)$. By inspecting $\partial \text{SINR}_{CBf,Q}^\infty(X_d)/\partial \rho_{C,Q}$ and $\partial \text{SINR}_{CBf,Q}^\infty(X_t)/\partial \rho_{C,Q}$ we can see that that $\text{SINR}_{CBf,Q}^\infty(x_d^*)$ is continuously differentiable for the region, $\rho_{C,Q} \in [0, \rho_{th})$ and $\rho_{C,Q} \in [\rho_{th}, \infty)$, respectively. To show $\text{SINR}_{CBf,Q}^\infty(x_d^*)$ is continuously differentiable for $\rho_{C,Q} \in [0, \infty)$ we need to establish $\partial \text{SINR}_{CBf,Q}^\infty(x_d^*)/\partial \rho_{C,Q}$ to be continuous at $\rho_{C,Q} = \rho_{th}$, or equivalently

$$\lim_{\rho_{C,Q} \rightarrow \rho_{th}^-} \frac{\partial \text{SINR}_{CBf,Q}^\infty(X_d)}{\partial \rho_{C,Q}} = \lim_{\rho_{C,Q} \rightarrow \rho_{th}^+} \frac{\partial \text{SINR}_{CBf,Q}^\infty(X_t)}{\partial \rho_{C,Q}} = \left. \frac{\partial \text{SINR}_{CBf,Q}^\infty(X_t)}{\partial \rho_{C,Q}} \right|_{\rho_{C,Q} = \rho_{th}} \quad (39)$$

When $\rho_{C,Q} \rightarrow \rho_{th}^-$, $X_d \rightarrow X_t$ and therefore the denominator of $\partial \text{SINR}_{CBf,Q}^\infty(X_d)/\partial \rho_{C,Q}$ and $\partial \text{SINR}_{CBf,Q}^\infty(X_t)/\partial \rho_{C,Q}$ are

equal. Let $\mathcal{N}(f)$ denote the numerator of f . As $X_d \rightarrow X_t$, we have

$$\begin{aligned} \lim_{\rho_{C,Q} \rightarrow \rho_{th}^-} \mathcal{N}(\partial \text{SINR}_{CBf,Q}^\infty(X_d)/\partial \rho_{C,Q}) &= [\beta(G_2' + \epsilon G_3')(1/\gamma_d + 1 + \epsilon - (1 - X_t)) + \beta\epsilon(1 - X_t)(G_2 G_3' - G_3 G_2') \\ &\quad - \rho_{th}(1 - X_t)G_2'] \Gamma_Q(1 - X_t) - \lim_{\rho_{C,Q} \rightarrow \rho_{th}^-} X_d'(\beta G_2 + \beta\epsilon G_3 + \rho)\gamma_e \\ &= \mathcal{N}\left(\left.\frac{\partial \text{SINR}_{CBf,Q}^\infty(X_t)}{\partial \rho_{C,Q}}\right|_{\rho_{C,Q}=\rho_{th}}\right) - \lim_{\rho_{C,Q} \rightarrow \rho_{th}^-} X_d'(\beta G_2 + \beta\epsilon G_3 + \rho)\gamma_e, \end{aligned}$$

where $X_d' = \partial X_d / \partial \rho_{C,Q}$. We should note that $\lim_{\rho_{C,Q} \rightarrow \rho_{th}^-} X_d' = -\frac{1}{2}\epsilon G_3' \frac{1-X_t}{\frac{1}{\gamma_d}+1+\epsilon} \neq 0$. This shows that x_d^* is not continuously differentiable over $\rho_{C,Q}$. Now let us look at

$$\begin{aligned} \lim_{\rho_{C,Q} \rightarrow \rho_{th}^-} \gamma_e &= \frac{1}{\gamma_d} + 1 + \epsilon + \epsilon(G_3 - 1) \left(-1 + \frac{1}{X_t}\right) \\ &= \frac{1}{X_t} \left[\left(\frac{1}{\gamma_d} + 1\right) X_t + \epsilon(2X_t - 1) - \epsilon G_3(X_t - 1) \right] = 0 \end{aligned}$$

since as $\rho_{C,Q} \rightarrow \rho_{th}^-$, from the (equivalent) condition $\epsilon = \epsilon_{th}$, the term in the bracket becomes 0. This concludes (39) and therefore $\text{SINR}_{CBf,Q}^\infty(x_d^*)$ is continuously differentiable for $\rho_{C,Q} \in [0, \infty)$.

By using the property above and the facts that the $\text{SINR}_{CBf,Q}^\infty(X_d)$ and $\text{SINR}_{CBf,Q}^\infty(X_t)$ are quasi-concave (unimodal), we can determine the optimal $\rho_{C,Q}^*$ and x_d^* jointly as described in Algorithm 1. We can verify the steps 6-13 in

Algorithm 1 Calculate $\rho_{C,Q}^*$ and x_d^*

```

1: Compute  $\rho_{th}$ 
2: if  $\rho_{th} \leq 0$  then
3:    $x_d^* = X_t$ .
4:    $\rho_{C,Q}^* = \rho_{X_t}^\circ$ 
5: else
6:   Compute  $\rho_{X_t}^\circ$ 
7:   if  $\rho_{X_t}^\circ \geq \rho_{th}$  then
8:      $x_d^* = X_t$ 
9:      $\rho_{C,Q}^* = \rho_{X_t}^\circ$ 
10:  else
11:     $x_d^* = X_d$ 
12:     $\rho_{C,Q}^* = \rho_{X_d}^\circ$ 
13:  end if
14: end if

```

the algorithm by using the following arguments: If $\rho_{X_t}^\circ > \rho_{th}$, then the derivate of $\text{SINR}_{CBf,Q}^\infty(X_t)$ is positive at $\rho_{C,Q} = \rho_{th}$ because $\text{SINR}_{CBf,Q}^\infty(X_t)$ is quasi-concave. Since the $\text{SINR}_{CBf,Q}^\infty(x_d^*)$ is continuously differentiable, then the derivative of $\text{SINR}_{CBf,Q}^\infty(X_d)$ is also positive when $\rho_{C,Q} \rightarrow \rho_{th}$. Since $\text{SINR}_{CBf,Q}^\infty(X_d)$ is also quasi-concave, consequently $\text{SINR}_{CBf,Q}^\infty(X_d)$ is increasing for $\rho_{C,Q} \in [0, \rho_{th})$. This implies that $\rho_{C,Q}^* = \rho_{X_t}^\circ$. Similar types of arguments can be also used to verify that if $\rho_{X_t}^\circ < \rho_{th}$ then $\rho_{C,Q}^* = \rho_{X_d}^\circ$.

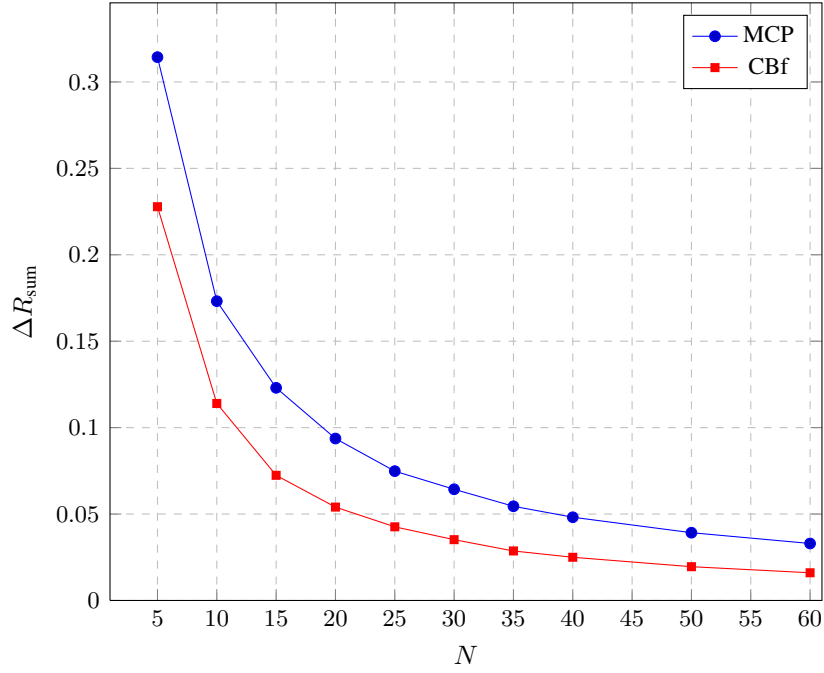


Fig. 5. The total sum-rate difference for different system dimensions with $\beta = 0.6$, $\epsilon = 0.5$, $\gamma_d = 10$ dB and $\bar{B}_t = 4$.

C. Numerical Results

The first two figures in this section are obtained by using a similar procedure to that followed in the analog feedback case. Figure 5 shows how well the limiting sum-rate (equivalently the limiting SINR) approximates the finite-size system sum-rate. The optimal regularization parameter and bit allocation are applied in computing the limiting and average sum-rates. As N grows, the normalized sum-rate difference become smaller. For $N = 60, K = 36$, it is already about 3.1% and 1.6% for MCP and CBf, respectively. Figure 6 shows the average sum-rate difference, with a fixed regularization parameter, between the system that uses $B_{d,FS}^*$ and \bar{B}_d^* to feed back the direct channel states. $B_{d,FS}^*$ denotes the optimal bit allocation of the finite-size system. For each channel realization, it is obtained by a grid search. With $N = 10, K = 6$, the maximum normalized average sum-rate difference reaches 0.22% for MCP. It is about four-times bigger for CBf, which is approximately 0.86%. Thus, from those simulations, similar to the analog feedback case, the conclusions we can reach for the limiting regime are actually useful for the finite system case.

In the following, we present numerical simulations that show the behavior of the limiting SINR and optimal bit allocation for MCP and CBf as ϵ varies. The optimal bit allocation is illustrated in Figure 7. As shown in Section IV, the optimal B_d for MCP is decreasing in ϵ and $B_d^* = B_t$ when $\epsilon = 0$. For CBf, $B_d^* = B_t$ when $\epsilon \leq 0.19$, and after that decreases as ϵ grows. Overall, for given ϵ , B_d^* for CBf is larger than for MCP, implying the quality of the direct channel information is more important for CBf.

In Figure 7, the optimal values for the regularization parameter and bit allocation are used. From that figure, it is obvious that $\text{SINR}_{\text{CBFQ}}^\infty$ decreases as ϵ increases. In the case of MCP, as predicted by the analysis, the limiting

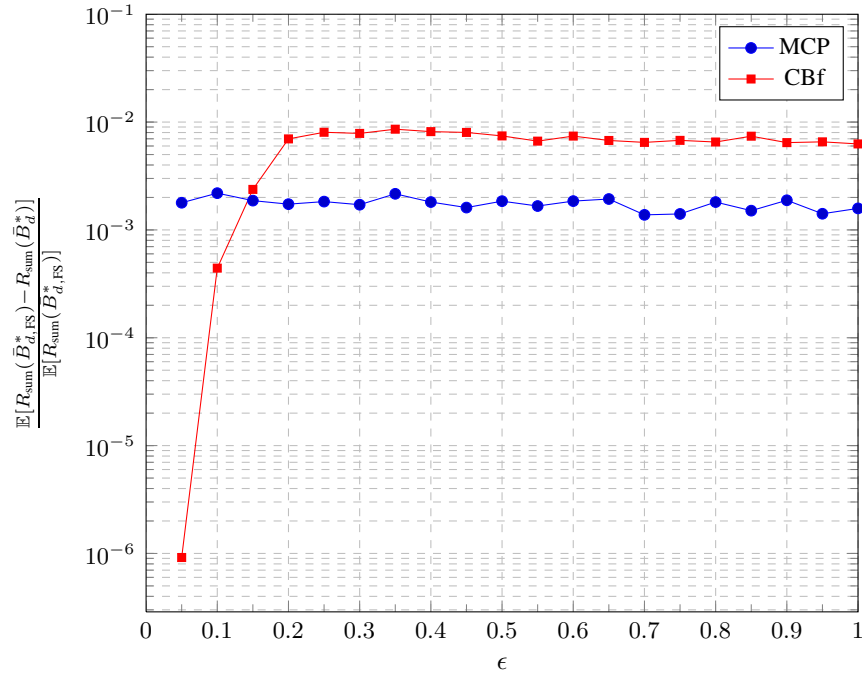


Fig. 6. The (normalized) average sum-rate difference of the finite-size system by using the $\bar{B}_{d,\text{FS}}^*$ and \bar{B}_d^* with $N = 10$, $\beta = 0.6$, $\gamma_d = 10$ dB and $\bar{B}_t = 4$.

SINR is decreasing until $\epsilon_{\text{M,RVQ}}^* \approx 0.72$ and is increasing after that point. By comparing the limiting SINR for both cooperation schemes, it is also interesting to see that for some values of ϵ , i.e., in the interval when CBf has $\bar{B}_c^* = 0$, the CBf slightly outperforms MCP. We should note that within the current scheme, when $\bar{B}_c^* = 0$, CBf and MCP are not the same as single-cell processing (SCP): under RVQ, there is still a quantization vector in the codebook that is used to represent the cross channel (although it is uncorrelated with the actual channel vector being quantized).

Motivated by the above facts, we investigate whether SCP provides some advantages over MCP and CBf for some (low) values of ϵ . In SCP, we use $B_{k,j,j} = B_t$ bits ($\forall k, j$) to quantize the direct channel. The cross channels in the precoder are represented by vectors with zero entries. By following the steps in deriving Theorem 3 and 6, we can show that the limiting SINR is given by

$$\text{SINR}_{\text{SCP,Q}}^\infty = \gamma_e g(\beta, \rho_s) \frac{1 + \frac{\rho_s}{\beta} (1 + g(\beta, \rho_s))^2}{\gamma_e + (1 + g(\beta, \rho_s))^2},$$

where $\rho_s = N^{-1}\alpha$ and $\gamma_e = \frac{1-2^{-B_t}}{2^{-B_t} + \epsilon + \frac{1}{\gamma_d}}$. It follows that the optimal ρ_s maximizing $\text{SINR}_{\text{SCP,Q}}^\infty$ is $\rho_s^* = \frac{\beta}{\gamma_e}$ and the corresponding the limiting SINR is $\text{SINR}_{\text{SCP,Q}}^{*,\infty} = g(\beta, \rho_s^*)$.

From Figure 7, it is obvious that the SCP outperforms MCP and CBf for some values of ϵ , that is, $\epsilon \leq 0.13$. Surprisingly, the CBf is still beaten by SCP until $\epsilon \approx 0.82$. This means that the SCP still gives advantages over the CBf even in a quite strong interference regime with this level of feedback.

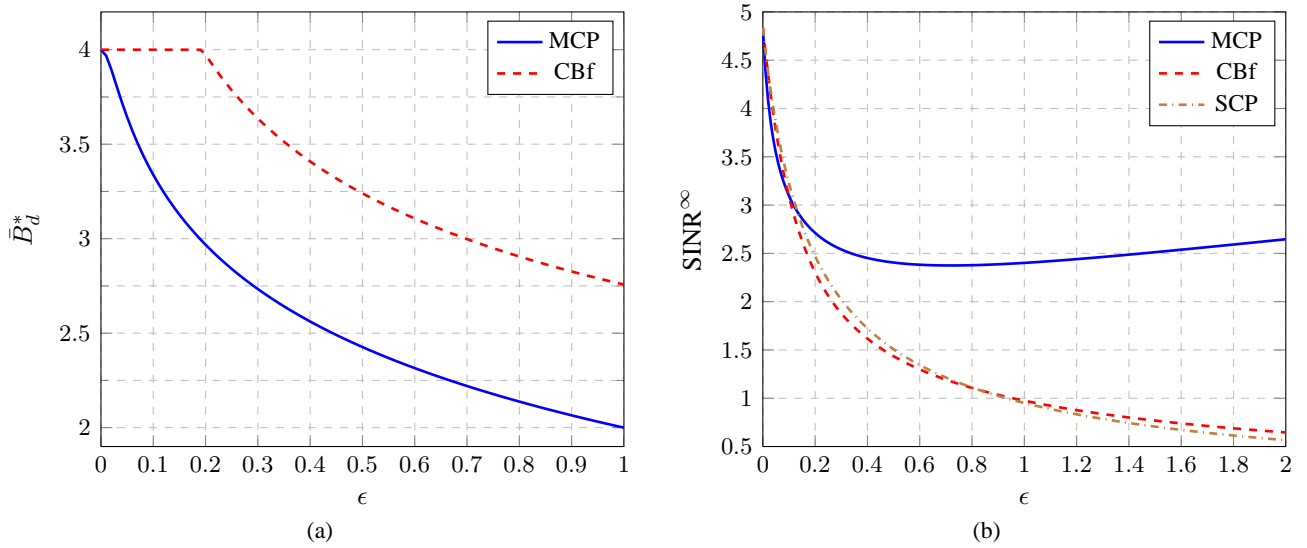


Fig. 7. (a) Optimal bit allocation vs ϵ (b) Limiting SINR vs. ϵ . Parameters: $\gamma_d=10$ dB, $\bar{B}_t = 4$.

V. ANALOG VS. DIGITAL FEEDBACK

In this section we will compare the performance of the analog and quantized feedback for each cooperation scheme. For the quantized feedback, we follow the approach in [14], [21], [23], [38] that translates feedback bits to symbols for a fair comparison with the analog feedback. In this regard, there are two approaches [14]:

- 1) By assuming that the feedback channel is error free and transmitted at the uplink rate (even though this assumption could be unrealistic in practice), we can write

$$\bar{B}_t = \frac{B_t}{N} = 2\kappa \log_2 (1 + (1 + \epsilon)\gamma_u). \quad (40)$$

This approach is introduced in [21], [23]. (40) is obtained by assuming that each feedback bit is received by both base stations in different cells where the path-gains from a user to its own BS and other BS are different i.e, 1 and ϵ respectively. We can think the feedback transmission from a user to both BSs as a Single-Input Multi-Output (SIMO) system. The BSs linearly combine the feedback signal from the user and the corresponding maximum SINR is $(1 + \epsilon)\gamma_u$ (see [39]). The pre-log factor $2\kappa N$ for B_t in (40) presents the channel uses (symbols) for transmitting the feedback bits which are the same as those for the analog feedback. κ follows the discussion in Section II-C. Our approach is different from the approach in [14] in which the user k in cell j sends the feedbacks only to its own BS j . In that case, (40) becomes $\bar{B}_t = 2\kappa \log_2 (1 + \gamma_u)$.

- 2) Following [38], the second approach translates the feedback bits to symbols based on the modulation scheme used in the feedback transmission. In the analog feedback, the feedback takes $2\kappa N$ channel uses per user. Let η be a conversion factor that links the bits and symbols and it depends on the modulation scheme. As

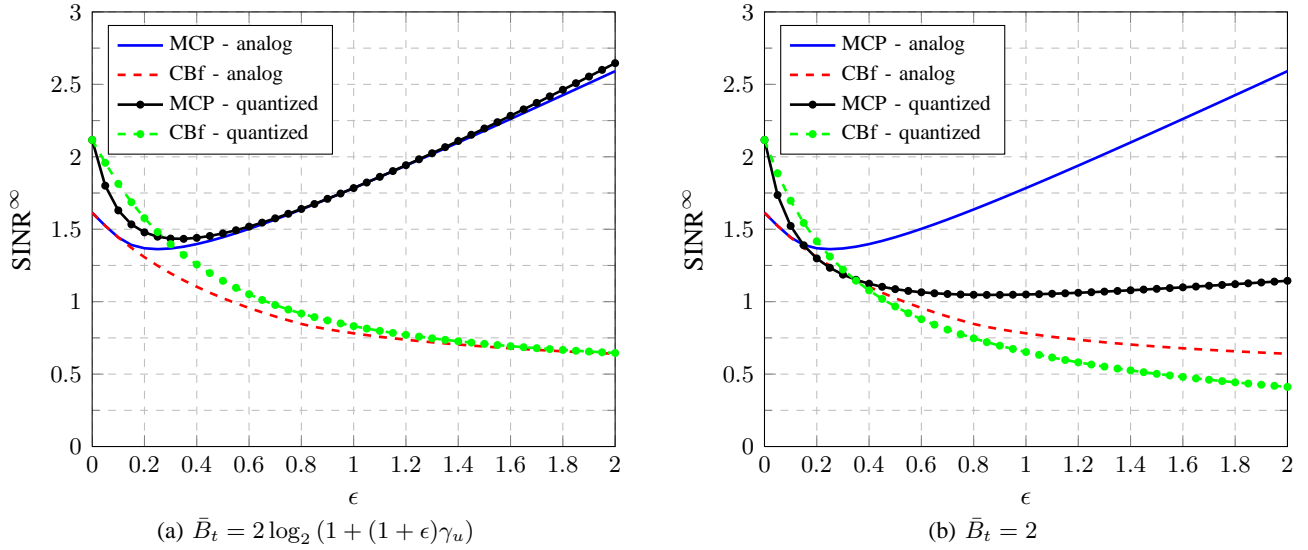


Fig. 8. The comparison of the limiting SINR of the analog and quantized feedback for different cooperation schemes. Parameters: $\beta = 0.6$, $\gamma_d = 10$ dB, $\gamma_u = 0$ dB

an example, for the binary phase shift keying (BPSK), $\eta = 1$. Thus, we can write (see also [14])

$$\eta B_t = 2\kappa N. \quad (41)$$

We should note that using this approach, for a fixed κ there is no link between \bar{B}_t and γ_u as we can see in (40).

Let us assume that $\kappa = 1$. Thus, with the first approach, we have $X_t = 2^{-\bar{B}_t} = \frac{1}{(1+(1+\epsilon)\gamma_u)^2}$. The comparison of the limiting SINR based on the analog and quantized feedback for MCP and CBf can be seen in Figure 8(a). It shows that the quantized feedback beats the analog feedback in both MCP and CBf for ϵ less than about 1. A similar situation still occurs for CBf even for $\epsilon \in [0, 2]$. The opposite happens for MCP when ϵ is above 1.5. The comparison of the analog and quantized feedback with the second approach, also with $\kappa = 1$, is illustrated in Figure 8(b). Similar to the previous, one can see that the quantized feedback outperforms the analog feedback if ϵ is below a certain threshold. Otherwise, the analog feedback gives better performance. Those observations can be explained by verifying whether the feedback scheme that provides better CSIT will give a better performance. This is easier to check by looking at the MCP scheme because from our discussions in Section III and IV, its performance can be measured by the total CSIT quality, i.e., $\omega_c + \omega_d$ in the analog feedback and $(1 + \epsilon)d^2$ in the digital feedback. Plotting those over ϵ , not shown here, will give the same behaviors for the MCP as we observed in Figure 8. Thus, from our simulations above, the CSIT quality of the quantized feedback is better than that of analog feedback when the cross channel gain is below a certain threshold. The above plots also confirm that more feedback resources will increase the system performance: for a fixed $\gamma_u = 0$ dB, \bar{B}_t in the left plot is larger than that in the right plot and hence gives a higher (limiting) SINR for the quantized feedback scheme.

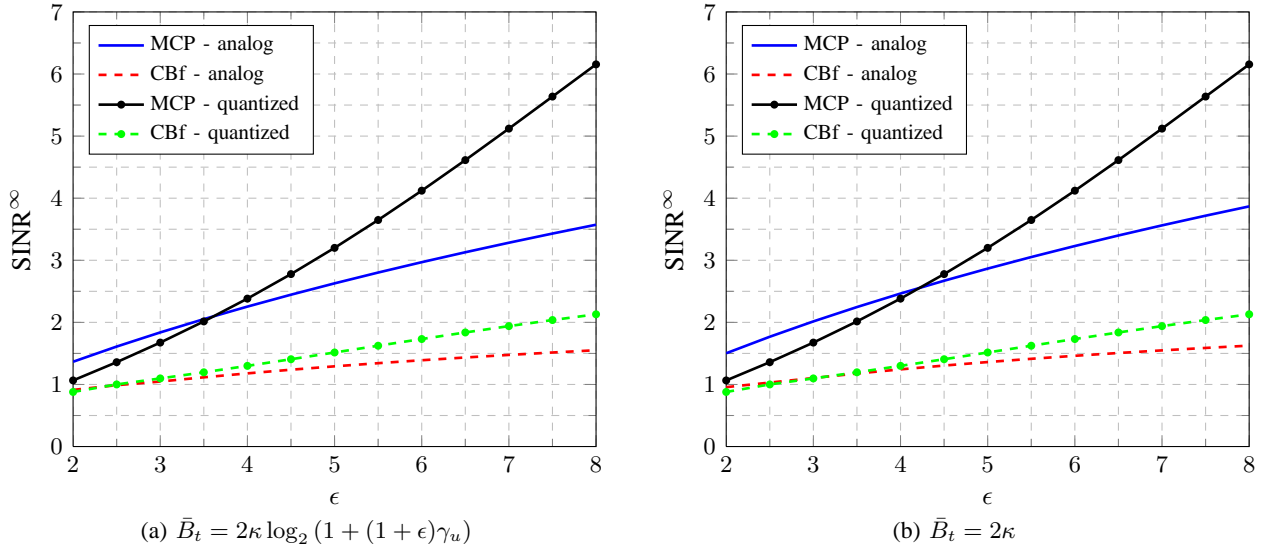


Fig. 9. The comparison of the limiting SINR of the analog and quantized feedback for different cooperation schemes vs. the feedback rates. Parameters: $\beta = 0.6$, $\epsilon = 0.6$, $\gamma_d = 10$ dB, $\gamma_u = 0$ dB

Figure 9 depicts the limiting SINR of the analog and quantized feedback for different values of feedback rate. For the analog feedback, the values of feedback rate/bit is converted by using the previous approaches: $\kappa = \frac{\bar{B}_t}{2\log_2(1+(1+\epsilon)\gamma_u)}$ and $\kappa = \bar{B}_t/2$ respectively. For MCP, we can see that initially the analog feedback scheme outperforms the quantized feedback in both plots. However, after a certain value (threshold) of \bar{B}_t , the opposite happens. A similar observation also holds for the CBf scheme. The explanations for those phenomena follow the discussions for Figure 8. We should note that in generating the figures, the values for \bar{B}_t are already determined. So, the limiting SINRs for the digital feedback are the same in both sub-figures. For the analog feedback, since κ with the approach (41) is larger (with $\gamma_u = 0$ dB) than that with the approach (40), then the training period in the former is longer and will result in a better CSIT. Thus, the limiting SINRs for the analog feedback in Figure 9(b) are larger compared to those in 9(a).

VI. CONCLUSION

In this paper, we perform feedback optimization for the analog and quantized feedback schemes in a symmetric two-cell network with different levels of cooperation between base stations. In both cooperation schemes, it is shown that more resources, uplink transmit power in the case of analog feedback or feedback bits in the case of quantized feedback, are allocated to feeding back the interfering channel information as the interfering channel gain increases. Moreover, if the interfering channel gain is below a certain threshold, the conventional network with no cooperation between base stations is preferable. Our analysis also shows that the limiting SINR for MCP, in both analog and quantized feedback, improves in ϵ if ϵ is above certain threshold. This also implies that above that threshold the (total) quality of the channel at the base stations is also getting better. Although our analysis is performed in the asymptotic regime, our numerical results hint to their validity in the finite-size system cases.

Future works could consider a more general channel model such as analog feedback through MAC channels. Furthermore, feedback reduction problems in which the users or groups of users have different path-loss gains can be interesting to explore.

APPENDIX I

SOME RESULTS IN RANDOM MATRIX THEORY

For the clarity in presentation, in this section we will list some results in random matrix theory that will be used to derive the large system results in this work.

Lemma 1 ([40, Lemma 1]). *Let \mathbf{A} be a deterministic $N \times N$ complex matrix with uniformly bounded spectral radius for all N . Let $\mathbf{q} = \frac{1}{\sqrt{N}}[q_1, q_2, \dots, q_N]^T$ where the q_i 's are i.i.d with zero mean, unit variance and finite eight moment. Let \mathbf{r} be a similar vector independent of \mathbf{q} . Then, we have*

$$\mathbf{q}\mathbf{A}\mathbf{q}^H - \frac{1}{N}\text{Tr}(\mathbf{A}) \xrightarrow{a.s.} 0, \text{ and } \mathbf{q}\mathbf{A}\mathbf{r}^H \xrightarrow{a.s.} 0.$$

Theorem 8 ([41]). *Let \mathbf{H} be a $[cN] \times [dN]$ random matrix with independent entries $[\mathbf{H}]_{ij}$ which are zero mean and variance $\mathbb{E}[|[\mathbf{H}]_{ij}|^2] = N^{-1}P_{ij}$, such that P_{ij} are uniformly bounded from above. For each N , let*

$$v_N(x, y) : [0, c] \times [0, d] \rightarrow \mathbb{R}$$

be the variance profile function given by

$$v_N(x, y) = P_{ij}, \quad \frac{i}{N} \leq x \leq \frac{i+1}{N}, \quad \frac{j}{N} \leq y \leq \frac{j+1}{N}.$$

Suppose that $v_N(x, y)$ converges uniformly to a limiting bounded function $v(x, y)$. Then, for each $a, b \in [0, c]$, $a < b$, and $z \in \mathbb{C}^+$

$$\frac{1}{N} \sum_{i=[aN]}^{[bN]} \left[(\mathbf{H}\mathbf{H}^H - z\mathbf{I})^{-1} \right]_{ii} \xrightarrow{i.p.} \int_a^b u(x, z) \, dz$$

where $u(x, z)$ satisfies

$$u(x, z) = \frac{1}{-z + \int_0^d \frac{v(x, y) dy}{1 + \int_0^c u(w, z) v(w, y) dw}}$$

for every $x \in [0, c]$. The solution always exists and is unique in the class of functions $u(x, z) \geq 0$, analytic on $z \in \mathbb{C}^+$ and continuous on $x \in [0, c]$. Moreover, almost surely, the empirical eigenvalue distribution of $\mathbf{H}\mathbf{H}^H$ converges weakly to a limiting distribution whose Stieltjes transform is given by $\int_0^1 u(x, z) \, dx$

In the theorem above x -axis and y -axis refer to the rows and columns of the matrix \mathbf{H} , respectively.

APPENDIX II

LARGE SYSTEM RESULTS FOR THE NETWORK MIMO

First, we will expand the SINR expression in (2). Let $\Phi_{k,j} = \text{diag}\{\phi_{k,j,1}, \phi_{k,j,2}\}$. Based on (1) we can write $\mathbf{h}_{k,j} = \hat{\mathbf{h}}_{k,j} \Phi_{k,j}^{\frac{1}{2}} + \tilde{\mathbf{h}}_{k,j}$. Consequently, the SINR can be expressed as

$$\text{SINR}_{k,j} = \frac{c^2 \left| (\hat{\mathbf{h}}_{k,j} \Phi_{k,j}^{\frac{1}{2}} + \tilde{\mathbf{h}}_{k,j}) (\hat{\mathbf{H}}^H \hat{\mathbf{H}} + \alpha \mathbf{I})^{-1} \hat{\mathbf{h}}_{k,j}^H \right|^2}{c^2 (\hat{\mathbf{h}}_{k,j} \Phi_{k,j}^{\frac{1}{2}} + \tilde{\mathbf{h}}_{k,j}) (\hat{\mathbf{H}}^H \hat{\mathbf{H}} + \alpha \mathbf{I})^{-1} \hat{\mathbf{H}}_{k,j}^H \hat{\mathbf{H}}_{k,j} (\hat{\mathbf{H}}^H \hat{\mathbf{H}} + \alpha \mathbf{I})^{-1} (\hat{\mathbf{h}}_{k,j} \Phi_{k,j}^{\frac{1}{2}} + \tilde{\mathbf{h}}_{k,j})^H + \sigma_d^2}. \quad (42)$$

It holds that $(\hat{\mathbf{H}}^H \hat{\mathbf{H}} + \alpha \mathbf{I})^{-1} = (\hat{\mathbf{H}}_{k,j}^H \hat{\mathbf{H}}_{k,j} + \hat{\mathbf{h}}_{k,j}^H \hat{\mathbf{h}}_{k,j} + \alpha \mathbf{I})^{-1}$. By applying the matrix inversion lemma (MIL) to the RHS of the (previous) equation, we obtain

$$(\hat{\mathbf{H}}^H \hat{\mathbf{H}} + \alpha \mathbf{I})^{-1} = (\hat{\mathbf{H}}_{k,j}^H \hat{\mathbf{H}}_{k,j} + \alpha \mathbf{I})^{-1} - \frac{(\hat{\mathbf{H}}_{k,j}^H \hat{\mathbf{H}}_{k,j} + \alpha \mathbf{I})^{-1} \hat{\mathbf{h}}_{k,j}^H \hat{\mathbf{h}}_{k,j} (\hat{\mathbf{H}}_{k,j}^H \hat{\mathbf{H}}_{k,j} + \alpha \mathbf{I})^{-1}}{1 + \hat{\mathbf{h}}_{k,j} (\hat{\mathbf{H}}_{k,j}^H \hat{\mathbf{H}}_{k,j} + \alpha \mathbf{I})^{-1} \hat{\mathbf{h}}_{k,j}^H}. \quad (43)$$

Let $\rho = \frac{\alpha}{N}$ and $\mathbf{O}_{k,j} = (\frac{1}{N} \hat{\mathbf{H}}_{k,j}^H \hat{\mathbf{H}}_{k,j} + \rho \mathbf{I})^{-1}$. Then, we can write (43) as $\frac{1}{N} \mathbf{Z}_{k,j}$, where

$$\mathbf{Z}_{k,j} = \mathbf{O}_{k,j} - \frac{\mathbf{O}_{k,j} \left(\frac{1}{N} \hat{\mathbf{h}}_{k,j}^H \hat{\mathbf{h}}_{k,j} \right) \mathbf{O}_{k,j}}{1 + \frac{1}{N} \hat{\mathbf{h}}_{k,j} \mathbf{O}_{k,j} \hat{\mathbf{h}}_{k,j}^H}.$$

Thus, (42) can be expressed as

$$\text{SINR}_{k,j} = \frac{c^2 \left| \frac{\check{A}_{k,j} + F_{k,j}}{1 + A_{k,j}} \right|^2}{c^2 (B_{k,j} + 2\Re[D_{k,j}] + E_{k,j}) + \sigma_d^2}, \quad (44)$$

where

$$\begin{aligned} \check{A}_{k,j} &= \frac{1}{N} \hat{\mathbf{h}}_{k,j} \Phi_{k,j}^{\frac{1}{2}} \mathbf{O}_{k,j} \hat{\mathbf{h}}_{k,j}^H \\ A_{k,j} &= \frac{1}{N} \hat{\mathbf{h}}_{k,j} \mathbf{O}_{k,j} \hat{\mathbf{h}}_{k,j}^H \\ F_{k,j} &= \frac{1}{N} \tilde{\mathbf{h}}_{k,j} \Phi_{k,j}^{\frac{1}{2}} \mathbf{O}_{k,j} \hat{\mathbf{h}}_{k,j}^H \\ B_{k,j} &= \frac{1}{N} \hat{\mathbf{h}}_{k,j} \Phi_{k,j}^{\frac{1}{2}} \mathbf{Z}_{k,j} \left(\frac{1}{N} \hat{\mathbf{H}}_{k,j}^H \hat{\mathbf{H}}_{k,j} \right) \mathbf{Z}_{k,j} \Phi_{k,j}^{\frac{1}{2}} \hat{\mathbf{h}}_{k,j}^H \\ D_{k,j} &= \frac{1}{N} \hat{\mathbf{h}}_{k,j} \Phi_{k,j}^{\frac{1}{2}} \mathbf{Z}_{k,j} \left(\frac{1}{N} \hat{\mathbf{H}}_{k,j}^H \hat{\mathbf{H}}_{k,j} \right) \mathbf{Z}_{k,j} \tilde{\mathbf{h}}_{k,j}^H \\ E_{k,j} &= \frac{1}{N} \tilde{\mathbf{h}}_{k,j} \mathbf{Z}_{k,j} \left(\frac{1}{N} \hat{\mathbf{H}}_{k,j}^H \hat{\mathbf{H}}_{k,j} \right) \mathbf{Z}_{k,j} \tilde{\mathbf{h}}_{k,j}^H. \end{aligned}$$

Note that for the analog feedback, $\Phi_{k,j} = \mathbf{I}, \forall k, j$. In the following subsections, the large system limit of each term in the SINR (44), for the analog and quantized feedback cases, will be derived. For brevity in the following presentation, we also denote $\mathbf{Q}_{k,j} = \mathbf{O}_{k,j} \left(\frac{1}{N} \hat{\mathbf{H}}_{k,j}^H \hat{\mathbf{H}}_{k,j} \right) \mathbf{O}_{k,j}$.

A. Proof of Theorem 1: Analog Feedback case

In the analog feedback case, as mentioned in Section III, $\hat{\mathbf{h}}_{k,i,j} \sim \mathcal{CN}(0, \omega_{ij} \mathbf{I}_N)$ and $\tilde{\mathbf{h}}_{k,i,j} \sim \mathcal{CN}(0, \delta_{ij} \mathbf{I}_N)$ are independent. We can rewrite those vectors respectively as

$$\hat{\mathbf{h}}_{k,j} = \mathbf{g}_{k,j} \mathbf{G}_{k,j}^{\frac{1}{2}} \text{ and } \tilde{\mathbf{h}}_{k,j} = \mathbf{d}_{k,j} \mathbf{D}_{k,j}^{\frac{1}{2}},$$

where $\mathbf{g}_{k,j} \sim \mathcal{CN}(0, \mathbf{I}_{2N})$ and $\mathbf{d}_{k,j} \sim \mathcal{CN}(0, \mathbf{I}_{2N})$ are independent. The diagonal matrices $\mathbf{G}_{k,j}$ and $\mathbf{D}_{k,j}$ are given by $\mathbf{G}_{k,j} = \text{diag}\{\omega_{j1} \mathbf{I}_N, \omega_{j2} \mathbf{I}_N\}$ and $\mathbf{D}_{k,j} = \text{diag}\{\delta_{j1} \mathbf{I}_N, \delta_{j2} \mathbf{I}_N\}$, respectively.

Since in the analysis below, we heavily use Theorem 8, let us define the asymptotic variance profile for the matrix $\frac{1}{N} \hat{\mathbf{H}}^H$ which is a $2N \times 2\beta N$ complex random matrix. Following Theorem 8, in our case, we have $x \in [0, 2]$, $y \in [0, 2\beta]$ and the asymptotic variance profile is given by

$$v(x, y) = \begin{cases} \omega_d & 0 \leq x < 1, 0 \leq y < \beta \\ \omega_c & 1 \leq x < 2, 0 \leq y < \beta \\ \omega_c & 0 \leq x < 1, \beta \leq y < 2\beta \\ \omega_d & 1 \leq x < 2, \beta \leq y < 2\beta. \end{cases}$$

In what follows, we will derive the large system limit for the terms in (44).

1) $\check{A}_{k,j}$: It can be rewritten as $\frac{1}{N} \mathbf{g}_{k,j} \mathbf{G}_{k,j}^{\frac{1}{2}} \mathbf{\Phi}_{k,j}^{\frac{1}{2}} \mathbf{O}_{k,j} \mathbf{G}_{k,j}^{\frac{1}{2}} \mathbf{g}_{k,j}^H$. Applying Lemma 1 yields

$$\check{A}_{k,j} - \frac{1}{N} \text{Tr} \left(\mathbf{G}_{k,j} \mathbf{\Phi}_{k,j}^{\frac{1}{2}} \mathbf{O}_{k,j} \right) \xrightarrow{a.s.} 0.$$

The second term in the LHS can be written as $\frac{1}{N} \left[\sum_{i=1}^N \omega_{j1} \sqrt{\phi_{k,j,1}} [\mathbf{O}_{k,j}]_{ii} + \sum_{i=N+1}^{2N} \omega_{j2} \sqrt{\phi_{k,j,2}} [\mathbf{O}_{k,j}]_{ii} \right]$. By applying Theorem 8, it converges in probability to

$$\omega_{j1} \sqrt{\phi_{k,j,1}} \int_0^1 u(x, -\rho) dx + \omega_{j2} \sqrt{\phi_{k,j,2}} \int_1^2 u(x, -\rho) dx,$$

where for $0 \leq x \leq 1$,

$$u(x, -\rho) = u_1 = \frac{1}{\rho + \frac{\beta \omega_d}{1+u_1 \omega_d + u_2 \omega_c} + \frac{\beta \omega_c}{1+u_1 \omega_c + u_2 \omega_d}}$$

and for $1 < x \leq 2$,

$$u(x, -\rho) = u_2 = \frac{1}{\rho + \frac{\beta \omega_c}{1+u_1 \omega_d + u_2 \omega_c} + \frac{\beta \omega_d}{1+u_1 \omega_c + u_2 \omega_d}}.$$

The solution of the equations above is $u_1 = u_2 = u$ where u is the positive solution of

$$u = \frac{1}{\rho + \frac{\beta(\omega_d + \omega_c)}{1+u(\omega_d + \omega_c)}}.$$

Let $g(\beta, \rho)$, be the solution of $g(\beta, \rho) = \left(\rho + \frac{\beta}{1+g(\beta, \rho)} \right)^{-1}$. Then, we can express u in term of $g(\beta, \rho)$ as

$$u = \frac{1}{\omega_d + \omega_c} g(\beta, \bar{\rho}), \quad \bar{\rho} = \frac{\rho}{\omega_d + \omega_c}.$$

We should note that $\omega_{j1} + \omega_{j2} = \omega_d + \omega_c$, $\forall j$. Thus,

$$\check{A}_{k,j} - \check{A}_{k,j}^{\infty} \xrightarrow{i.p.} 0, \text{ with } \check{A}_{k,j}^{\infty} = \frac{\sqrt{\phi_{k,j,1}\omega_{j1}} + \sqrt{\phi_{k,j,2}\omega_{j2}}}{\omega_d + \omega_c} g(\beta, \bar{\rho}).$$

Since in the current feedback scheme $\Phi_{k,j} = \mathbf{I}_{2N}$ then $\check{A}_{k,j}^{\infty} = g(\beta, \bar{\rho})$. Moreover, $\check{A}_{k,j}^{\infty} = \check{A}^{\infty}$ is the same for all users in both cells.

2) $A_{k,j}$: This term is $\check{A}_{k,j}$ with $\Phi_{k,i} = \mathbf{I}_{2N}$. Thus, it follows that $A_{k,j} - g(\beta, \bar{\rho}) \xrightarrow{i.p.} 0$.

3) $F_{k,j}$: It can be rewritten as $\frac{1}{N} \mathbf{d}_{k,j} D_{k,j}^{\frac{1}{2}} \mathbf{O}_{k,j} G_{k,j}^{\frac{1}{2}} \mathbf{g}_{k,j}^H$. Conditioning on $\hat{\mathbf{H}}_{k,j}$, it is obvious that $\mathbf{d}_{k,j}$, $\mathbf{g}_{k,j}$ and $D_{k,j}^{\frac{1}{2}} \mathbf{O}_{k,j} G_{k,j}^{\frac{1}{2}}$ are independent of each other. By Lemma 1, it follows that $F_{k,j} \xrightarrow{a.s.} 0$.

4) $D_{k,j}$: Expanding $D_{k,j}$, we have

$$\begin{aligned} D_{k,j} &= \frac{1}{N} \hat{\mathbf{h}}_{k,j} \Phi^{\frac{1}{2}} \mathbf{Q}_{k,j} \tilde{\mathbf{h}}_{k,j}^H + \frac{\check{A}_{k,j} F_{k,j}^* \left(\frac{1}{N} \hat{\mathbf{h}}_{k,j} \mathbf{Q}_{k,j} \hat{\mathbf{h}}_{k,j}^H \right)}{(1 + A_{k,j})^2} - \frac{F_{k,j}^* \left(\frac{1}{N} \hat{\mathbf{h}}_{k,j} \Phi^{\frac{1}{2}} \mathbf{Q}_{k,j} \hat{\mathbf{h}}_{k,j}^H \right)}{1 + A_{k,j}} - \frac{\check{A}_{k,j} \left(\frac{1}{N} \hat{\mathbf{h}}_{k,j} \mathbf{Q}_{k,j} \tilde{\mathbf{h}}_{k,j}^H \right)}{1 + A_{k,j}} \\ &= D_{k,j}^{(1)} + D_{k,j}^{(2)} - D_{k,j}^{(3)} - D_{k,j}^{(4)}. \end{aligned} \quad (45)$$

Following the arguments in 4), it can be checked that $D_{k,j}^{(1)} \xrightarrow{a.s.} 0$. Similarly, $D_{k,j}^{(4)} \xrightarrow{a.s.} 0$. Moreover, since $F_{k,j} \xrightarrow{a.s.} 0$ then it follows that $D_{k,j}^{(2)} \xrightarrow{a.s.} 0$ and $D_{k,j}^{(3)} \xrightarrow{a.s.} 0$. Combining the results yields $D_{k,j} \xrightarrow{a.s.} 0$.

5) $B_{k,j}$: It can be rewritten as

$$\begin{aligned} B_{k,j} &= \frac{1}{N} \hat{\mathbf{h}}_{k,j} \Phi^{\frac{1}{2}} \mathbf{Q}_{k,j} \Phi^{\frac{1}{2}} \hat{\mathbf{h}}_{k,j}^H + \frac{|\check{A}_{k,j}|^2 \left(\frac{1}{N} \hat{\mathbf{h}}_{k,j} \mathbf{Q}_{k,j} \hat{\mathbf{h}}_{k,j}^H \right)}{(1 + A_{k,j})^2} - \frac{2\Re \left[\check{A}_{k,j}^* \left(\frac{1}{N} \hat{\mathbf{h}}_{k,j} \Phi^{\frac{1}{2}} \mathbf{Q}_{k,j} \hat{\mathbf{h}}_{k,j}^H \right) \right]}{1 + A_{k,j}} \\ &= B_{k,j}^{(1)} + \frac{|\check{A}_{k,j}|^2 B_{k,j}^{(2)}}{(1 + A_{k,j})^2} - \frac{2\Re \left[\check{A}_{k,j}^* B_{k,j}^{(3)} \right]}{1 + A_{k,j}}. \end{aligned} \quad (46)$$

From Lemma 1, we can show $B_{k,j}^{(1)} - \frac{1}{N} \text{Tr}(\mathbf{G}_{k,j} \Phi_{k,j} \mathbf{Q}_{k,j}) \xrightarrow{a.s.} 0$. It can be shown that the following equality holds

$$(\mathbf{X}\mathbf{X}^H + \zeta \mathbf{I})^{-1} \mathbf{X}\mathbf{X}^H (\mathbf{X}\mathbf{X}^H + \zeta \mathbf{I})^{-1} = (\mathbf{X}\mathbf{X}^H + \zeta \mathbf{I})^{-1} + \zeta \frac{\partial}{\partial \zeta} (\mathbf{X}\mathbf{X}^H + \zeta \mathbf{I})^{-1}. \quad (47)$$

Thus, we have $\mathbf{Q}_{k,j} = \mathbf{O}_{k,j} + \rho \frac{\partial}{\partial \rho} \mathbf{O}_{k,j}$. By applying Theorem 8, we obtain

$$\frac{1}{N} \sum_{i=[aN]}^{[bN]} [\mathbf{Q}_{k,j}]_{ii} \xrightarrow{i.p.} \int_a^b u(x, -\rho) dx + \rho \frac{\partial}{\partial \rho} \int_a^b u(x, -\rho) dx.$$

Consequently, we can show $B_{k,j}^{(1)} - B_{k,j}^{(1),\infty} \xrightarrow{i.p.} 0$, where

$$B_{k,j}^{(1),\infty} = \frac{\omega_{j1}\phi_{k,j,1} + \omega_{j2}\phi_{k,j,2}}{\omega_d + \omega_c} \left[g(\beta, \bar{\rho}) + \bar{\rho} \frac{\partial}{\partial \bar{\rho}} g(\beta, \bar{\rho}) \right]. \quad (48)$$

Similarly, we can also show that $B_{k,j}^{(2)} - B_{k,j}^{(2),\infty} \xrightarrow{i.p.} 0$ and $B_{k,j}^{(3)} - B_{k,j}^{(3),\infty} \xrightarrow{i.p.} 0$, where

$$B_{k,j}^{(2),\infty} = g(\beta, \bar{\rho}) + \bar{\rho} \frac{\partial}{\partial \bar{\rho}} g(\beta, \bar{\rho}),$$

$$B_{k,j}^{(3),\infty} = \frac{\omega_j 1 \sqrt{\phi_{k,j,1}} + \omega_j 2 \sqrt{\phi_{k,j,2}}}{\omega_d + \omega_c} \left[g(\beta, \bar{\rho}) + \bar{\rho} \frac{\partial}{\partial \bar{\rho}} g(\beta, \bar{\rho}) \right].$$

For the analog feedback case, i.e., $\Phi_{k,j} = \mathbf{I}_{2N}$, it follows that $B_{k,j}^{(1),\infty} = B_{k,j}^{(2),\infty} = B_{k,j}^{(3),\infty}$. Therefore, $B_{k,j}$ converges in probability to

$$\frac{1}{(1 + g(\beta, \bar{\rho}))^2} \left[g(\beta, \bar{\rho}) + \bar{\rho} \frac{\partial}{\partial \bar{\rho}} g(\beta, \bar{\rho}) \right].$$

6) $E_{k,j}$: Expanding this term gives

$$E_{k,j} = \frac{1}{N} \tilde{\mathbf{h}}_{k,j} \mathbf{Q}_{k,j} \tilde{\mathbf{h}}_{k,j}^H - 2\Re \left[\frac{F_{k,j} \left(\frac{1}{N} \hat{\mathbf{h}}_{k,j} \mathbf{Q}_{k,j} \tilde{\mathbf{h}}_{k,j}^H \right)}{1 + A_{k,j}} \right] + \frac{|F_{k,j}|^2 \frac{1}{N} \hat{\mathbf{h}}_{k,j} \mathbf{Q}_{k,j} \hat{\mathbf{h}}_{k,j}^H}{(1 + A_{k,j})^2}$$

$$= E_{k,j}^{(1)} - E_{k,j}^{(2)} + E_{k,j}^{(3)}. \quad (49)$$

By using the previous results, we can show that $E_{k,j}^{(2)} \xrightarrow{a.s.} 0$ and $E_{k,j}^{(3)} \xrightarrow{i.p.} 0$. From Lemma 1, it follows that $E_{k,j}^{(1)} - \frac{1}{N} \text{Tr}(\mathbf{D}_{k,j} \mathbf{Q}_{k,j}) \xrightarrow{a.s.} 0$. Following the steps in obtaining $B_{k,j}^{(1),\infty}$, it is easy to show that $E_{k,j}^{(1)} - E_{k,j}^{(1),\infty} \xrightarrow{i.p.} 0$, where

$$E_{k,j}^{(1),\infty} = \frac{\delta_{k,j,1} + \delta_{k,j,2}}{\omega_d + \omega_c} \left[g(\beta, \bar{\rho}) + \bar{\rho} \frac{\partial}{\partial \bar{\rho}} g(\beta, \bar{\rho}) \right].$$

Thus, we have $E_{k,j} - E_{k,j}^{(1),\infty} \xrightarrow{i.p.} 0$.

7) c^2 : The denominator of c^2 can be written as follows

$$\frac{1}{N} \text{Tr} \left(\left(\frac{1}{N} \hat{\mathbf{H}}^H \hat{\mathbf{H}} + \rho \mathbf{I} \right)^{-2} \frac{1}{N} \hat{\mathbf{H}}^H \hat{\mathbf{H}} \right) = \int \frac{\lambda}{(\lambda + \rho)^2} dF_{\hat{\mathbf{H}}^H \hat{\mathbf{H}}}(\lambda),$$

where $F_{\hat{\mathbf{H}}^H \hat{\mathbf{H}}}$ is the empirical eigenvalue distribution of $\hat{\mathbf{H}}^H \hat{\mathbf{H}}$. From Theorem 8, $F_{\hat{\mathbf{H}}^H \hat{\mathbf{H}}}$ converges almost surely to a limiting distribution G^* whose Stieltjes transform $m(z) = \int_0^\infty \frac{1}{\lambda - z} dG^*(\lambda) = \int_0^1 u(x, z) dx$. Therefore,

$$\int \frac{\lambda}{(\lambda + \rho)^2} dF_{\hat{\mathbf{H}}^H \hat{\mathbf{H}}}(\lambda) = \int \frac{1}{\lambda + \rho} + \rho \frac{\partial}{\partial \rho} \frac{1}{\lambda + \rho} dF_{\hat{\mathbf{H}}^H \hat{\mathbf{H}}}(\lambda)$$

$$\xrightarrow{a.s.} m(-\rho) + \rho \frac{\partial}{\partial \rho} m(-\rho)$$

$$= \int_0^1 u(x, -\rho) + \rho \frac{\partial}{\partial \rho} u(x, -\rho) dx. \quad (50)$$

Previously, we have shown that $\int_0^1 u(x, -\rho) = 2(\omega_d + \omega_c)^{-1} g(\beta, \bar{\rho})$ with $\bar{\rho} = 2\rho(\omega_d + \omega_c)^{-1}$. Hence, (50) is equal to $2(\omega_d + \omega_c)^{-1} \left(g(\beta, \bar{\rho}) + \bar{\rho} \frac{\partial}{\partial \bar{\rho}} g(\beta, \bar{\rho}) \right)$ and the large system result for c^2 is given by

$$c^2 - \frac{\frac{1}{2}(\omega_d + \omega_c) P_t}{g(\beta, \bar{\rho}) + \bar{\rho} \frac{\partial}{\partial \bar{\rho}} g(\beta, \bar{\rho})} \xrightarrow{a.s.} 0.$$

The large system results in 1) - 3) and 7) show that the signal strength, i.e, the numerator of (44), converges to

$$\frac{(\omega_d + \omega_c)Pg^2(\beta, \bar{\rho})}{(1 + g(\beta, \bar{\rho}))^2 \left(g(\beta, \bar{\rho}) + \bar{\rho} \frac{\partial}{\partial \bar{\rho}} g(\beta, \bar{\rho}) \right)}, \quad (51)$$

where we already substitute $P = \frac{1}{2}P_t$. Similarly, it follows that the interference (energy) converges to

$$\frac{P}{(1 + g(\beta, \bar{\rho}))^2} \left(\omega_d + \omega_c - (\delta_d + \delta_c) (1 + g(\beta, \bar{\rho}))^2 \right). \quad (52)$$

To simplify the expression for the limiting $\text{SINR}_{k,j}$, we need the following result (see [37])

$$g(\beta, \bar{\rho}) + \bar{\rho} \frac{\partial}{\partial \bar{\rho}} g(\beta, \bar{\rho}) = \frac{\beta g(\beta, \bar{\rho})}{\beta + \bar{\rho}(1 + g(\beta, \bar{\rho}))^2}.$$

By combining the large system results and also denoting $\rho_{\text{M,AF}} = \bar{\rho}$, we can express the limiting SINR as in (13). This completes the proof.

B. Proof of Theorem 3: Quantized feedback (via RVQ) case

Since the $\phi_{k,j,i}$ is a random variable, while it is not in the analog feedback, the derivation for the limiting SINR is quite different from the previous subsection. For a given $2N \times 2N$ matrix \mathbf{X} , we can partition it as follows

$$\mathbf{X}_{k,j} = \begin{bmatrix} \mathbf{X}_{k,j}^{11} & \mathbf{X}_{k,j}^{12} \\ \mathbf{X}_{k,j}^{21} & \mathbf{X}_{k,j}^{22} \end{bmatrix},$$

where $\mathbf{X}_{k,j}^{11} = [\mathbf{X}_{k,j}]_{lm}, l = 1, \dots, N, m = 1, \dots, N$, $\mathbf{X}_{k,j}^{12} = [\mathbf{X}_{k,j}]_{lm}, l = 1, \dots, N, m = N+1, \dots, 2N$, $\mathbf{X}_{k,j}^{21} = [\mathbf{X}_{k,j}]_{lm}, l = N+1, \dots, 2N, m = 1, \dots, N$, and $\mathbf{X}_{k,j}^{22} = [\mathbf{X}_{k,j}]_{lm}, l = N+1, \dots, 2N, m = N+1, \dots, 2N$.

In the following, we derive the large system limit for each term in the SINR.

1) $\check{A}_{k,j}$: We can write $\check{A}_{k,j}$ as

$$\check{A}_{k,j} = \frac{1}{N} \left(\phi_{k,j,1}^{\frac{1}{2}} \hat{\mathbf{h}}_{k,j,1} \mathbf{O}_{k,j}^{11} \hat{\mathbf{h}}_{k,j,1}^H + \phi_{k,j,1}^{\frac{1}{2}} \hat{\mathbf{h}}_{k,j,1} \mathbf{O}_{k,j}^{12} \hat{\mathbf{h}}_{k,j,2}^H + \phi_{k,j,2}^{\frac{1}{2}} \hat{\mathbf{h}}_{k,j,2} \mathbf{O}_{k,j}^{21} \hat{\mathbf{h}}_{k,j,1}^H + \phi_{k,j,2}^{\frac{1}{2}} \hat{\mathbf{h}}_{k,j,2} \mathbf{O}_{k,j}^{22} \hat{\mathbf{h}}_{k,j,2}^H \right). \quad (53)$$

Since $\hat{\mathbf{h}}_{k,j,1}$ and $\hat{\mathbf{h}}_{k,j,2}$ are independent then the second and third terms converge almost surely to 0. For the first term

$$\frac{1}{N} \hat{\mathbf{h}}_{k,j,1} \mathbf{O}_{k,j}^{11} \hat{\mathbf{h}}_{k,j,1}^H - \frac{\omega_{j1}}{N} \text{Tr}(\mathbf{O}_{k,j}^{11}) \xrightarrow{a.s.} 0$$

or equivalently,

$$\frac{1}{N} \hat{\mathbf{h}}_{k,j,1} \mathbf{O}_{k,j}^{11} \hat{\mathbf{h}}_{k,j,1}^H - \frac{\omega_{j1}}{N} \sum_{i=1}^N [\mathbf{O}_{k,j}]_{ii} \xrightarrow{a.s.} 0.$$

By using the Girko's result (Theorem 8), we have

$$\frac{1}{N} \sum_{i=1}^N [\mathbf{O}_{k,j}]_{ii} \xrightarrow{i.p.} \frac{1}{1 + \epsilon} g(\beta, \bar{\rho}),$$

where $\bar{\rho} = \frac{\frac{1}{N}\alpha}{1+\epsilon}$. By using the same techniques as in [16], we can show that

$$\sqrt{\phi_{k,j,i}} = \sqrt{1 - \tau_{k,j,i}^2} \xrightarrow{L_2} \begin{cases} \sqrt{1 - 2^{-\bar{B}_d}} & j = i \\ \sqrt{1 - 2^{-\bar{B}_c}} & \text{otherwise.} \end{cases}$$

We should also note that the convergence in mean square sense implies the convergence in probability. By doing the same steps as for the last term of (53), we have

$$\check{A}_{k,j} - \frac{\sqrt{1 - 2^{-\bar{B}_d}} + \epsilon\sqrt{1 - 2^{-\bar{B}_c}}}{1 + \epsilon} g(\beta, \bar{\rho}) \xrightarrow{i.p.} 0.$$

2) $A_{k,j}$: This term is $\check{A}_{k,j}$ with $\Phi_{k,j} = \mathbf{I}_{2N}$. Hence, $A_{k,j} - g(\beta, \bar{\rho}) \xrightarrow{i.p.} 0$.

3) $F_{k,j}$: We can expand the term as follows

$$F_{k,j} = \frac{1}{N} \left(\tilde{\mathbf{h}}_{k,j,1} \mathbf{O}_{k,j}^{11} \hat{\mathbf{h}}_{k,j,1}^H + \tilde{\mathbf{h}}_{k,j,1} \mathbf{O}_{k,j}^{12} \hat{\mathbf{h}}_{k,j,2}^H + \tilde{\mathbf{h}}_{k,j,2} \mathbf{O}_{k,j}^{21} \hat{\mathbf{h}}_{k,j,1}^H + \tilde{\mathbf{h}}_{k,j,2} \mathbf{O}_{k,j}^{22} \hat{\mathbf{h}}_{k,j,2}^H \right) \quad (54)$$

By using the same steps as in deriving (65), it follows that each term on the RHS of the equation above converges in probability to 0. Hence, $F_{k,j} \xrightarrow{i.p.} 0$.

4) $B_{k,j}$: By following the representation (46) for $B_{k,j}$, we can express the first term on the RHS as

$$B_{k,j}^{(1)} = \frac{1}{N} \left(\phi_{k,j,1} \hat{\mathbf{h}}_{k,j,1} \mathbf{Q}_{k,j}^{11} \hat{\mathbf{h}}_{k,j,1}^H + \phi_{k,j,1} \hat{\mathbf{h}}_{k,j,1} \mathbf{Q}_{k,j}^{12} \hat{\mathbf{h}}_{k,j,2}^H + \phi_{k,j,2} \hat{\mathbf{h}}_{k,j,2} \mathbf{Q}_{k,j}^{21} \hat{\mathbf{h}}_{k,j,1}^H + \phi_{k,j,2} \hat{\mathbf{h}}_{k,j,2} \mathbf{Q}_{k,j}^{22} \hat{\mathbf{h}}_{k,j,2}^H \right).$$

The second term and the third term of the equation above converge (almost surely) to 0. For the first term,

$$\frac{1}{N} \hat{\mathbf{h}}_{k,j,1} \mathbf{Q}_{k,j}^{11} \hat{\mathbf{h}}_{k,j,1}^H - \frac{\omega_{j1}}{N} \text{Tr}(\mathbf{Q}_{k,j}^{11}) \xrightarrow{a.s.} 0.$$

From (47), we have $\mathbf{Q}_{k,j} = \mathbf{O}_{k,j} + \rho \frac{\partial}{\partial \rho} \mathbf{O}_{k,j}$. Hence, we can show

$$\frac{1}{N} \text{Tr}(\mathbf{Q}_{k,j}^{11}) = \frac{1}{N} \sum_{i=1}^N [\mathbf{Q}_{k,j}^{11}]_{ii} \xrightarrow{i.p.} \int_0^1 u(x, -\rho) dx + \rho \frac{\partial}{\partial \rho} \int_0^1 u(x, -\rho) dx = \frac{1}{1 + \epsilon} \left[g(\beta, \bar{\rho}) + \bar{\rho} \frac{\partial}{\partial \bar{\rho}} g(\beta, \bar{\rho}) \right].$$

By doing the same steps for the last term of $B_{k,j}^{(1)}$, it follows that

$$B_{k,j}^{(1)} - \frac{1 - 2^{-\bar{B}_d} + \epsilon(1 - 2^{-\bar{B}_c})}{1 + \epsilon} \left[g(\beta, \bar{\rho}) + \bar{\rho} \frac{\partial}{\partial \bar{\rho}} g(\beta, \bar{\rho}) \right] \xrightarrow{i.p.} 0.$$

Similarly, we can also show that

$$\begin{aligned} B_{k,j}^{(2)} - g(\beta, \bar{\rho}) + \bar{\rho} \frac{\partial}{\partial \bar{\rho}} g(\beta, \bar{\rho}) &\xrightarrow{i.p.} 0, \\ B_{k,j}^{(3)} - \frac{\sqrt{1 - 2^{-\bar{B}_d}} + \epsilon\sqrt{1 - 2^{-\bar{B}_c}}}{1 + \epsilon} \left[g(\beta, \bar{\rho}) + \bar{\rho} \frac{\partial}{\partial \bar{\rho}} g(\beta, \bar{\rho}) \right] &\xrightarrow{i.p.} 0. \end{aligned}$$

Combining the results together, we obtain

$$B_{k,j} - \left(\frac{1 - 2^{-\bar{B}_d} + \epsilon(1 - 2^{-\bar{B}_c})}{1 + \epsilon} - \frac{d^2(2 + g(\beta, \bar{\rho}))g(\beta, \bar{\rho})}{(1 + g(\beta, \bar{\rho}))^2} \right) \left[g(\beta, \bar{\rho}) + \bar{\rho} \frac{\partial}{\partial \bar{\rho}} g(\beta, \bar{\rho}) \right] \xrightarrow{i.p.} 0,$$

where

$$d = \frac{\sqrt{1 - 2^{-\bar{B}_d}} + \epsilon \sqrt{1 - 2^{-\bar{B}_c}}}{1 + \epsilon}.$$

5) $D_{k,j}$: We can expand $D_{k,j}$ as expressed in (45). Using the previous results, it follows immediately that $D_{k,j}^{(2)}$ and $D_{k,j}^{(3)}$ converge to 0. We can expand the first term as follows

$$D_{k,j}^{(1)} = \frac{1}{N} \left(\phi_{k,j,1}^{\frac{1}{2}} \hat{\mathbf{h}}_{k,j,1} \mathbf{Q}_{k,j}^{11} \tilde{\mathbf{h}}_{k,j,1}^H + \phi_{k,j,1}^{\frac{1}{2}} \hat{\mathbf{h}}_{k,j,1} \mathbf{Q}_{k,j}^{12} \tilde{\mathbf{h}}_{k,j,2}^H + \phi_{k,j,2}^{\frac{1}{2}} \hat{\mathbf{h}}_{k,j,2} \mathbf{Q}_{k,j}^{21} \tilde{\mathbf{h}}_{k,j,1}^H + \phi_{k,j,2}^{\frac{1}{2}} \hat{\mathbf{h}}_{k,j,2} \mathbf{Q}_{k,j}^{22} \tilde{\mathbf{h}}_{k,j,2}^H \right).$$

Again, by following the same steps as in deriving (65), each term converges in probability to 0 and hence $D_{k,j}^{(1)} \xrightarrow{i.p.} 0$. Similarly, $D_{k,j}^{(4)} \xrightarrow{i.p.} 0$. Therefore, $D_{k,j} \xrightarrow{i.p.} 0$.

6) $E_{k,j}$: The expansion of $E_{k,j}$ follows (49). By applying the previous results, $E_{k,j}^{(2)}$ and $E_{k,j}^{(3)}$ converge in probability to 0. $E_{k,j}^{(1)}$ can be rewritten as

$$E_{k,j}^{(1)} = \frac{1}{N} \left(\tilde{\mathbf{h}}_{k,j,1} \mathbf{Q}_{k,j}^{11} \tilde{\mathbf{h}}_{k,j,1}^H + \tilde{\mathbf{h}}_{k,j,1} \mathbf{Q}_{k,j}^{12} \tilde{\mathbf{h}}_{k,j,2}^H + \tilde{\mathbf{h}}_{k,j,2} \mathbf{Q}_{k,j}^{21} \tilde{\mathbf{h}}_{k,j,1}^H + \tilde{\mathbf{h}}_{k,j,2} \mathbf{Q}_{k,j}^{22} \tilde{\mathbf{h}}_{k,j,2}^H \right).$$

Since $\tilde{\mathbf{h}}_{k,j,1}$ and $\tilde{\mathbf{h}}_{k,j,2}$ are independent then the second and third term converge to 0. The first term in the equation above can be written as

$$\begin{aligned} \frac{1}{N} \tilde{\mathbf{h}}_{k,j,1} \mathbf{Q}_{k,j}^{11} \tilde{\mathbf{h}}_{k,j,1}^H &= \frac{\tau_{k,j,1}^2 \|\mathbf{h}_{k,j,1}\|^2}{N \|\mathbf{v}_{k,j,1} \Pi_{\hat{\mathbf{h}}_{k,j,1}}^\perp\|^2} \left(\mathbf{v}_{k,j,1} - \frac{(\mathbf{v}_{k,j,1} \hat{\mathbf{h}}_{k,j,1}^H) \hat{\mathbf{h}}_{k,j,1}}{\|\hat{\mathbf{h}}_{k,j,1}\|^2} \right) \mathbf{Q}_{k,j}^{11} \left(\mathbf{v}_{k,j,1} - \frac{(\mathbf{v}_{k,j,1} \hat{\mathbf{h}}_{k,j,1}^H) \hat{\mathbf{h}}_{k,j,1}}{\|\hat{\mathbf{h}}_{k,j,1}\|^2} \right)^H \\ &= \frac{\tau_{k,j,1}^2 \|\mathbf{h}_{k,j,1}\|^2}{\|\mathbf{v}_{k,j,1} \Pi_{\hat{\mathbf{h}}_{k,j,1}}^\perp\|^2} \left(\frac{1}{N} \mathbf{v}_{k,j,1} \mathbf{Q}_{k,j}^{11} \mathbf{v}_{k,j,1}^H + \frac{|\frac{1}{N} \mathbf{v}_{k,j,1} \hat{\mathbf{h}}_{k,j,1}^H|^2 \frac{1}{N} \hat{\mathbf{h}}_{k,j,1} \mathbf{Q}_{k,j}^{11} \hat{\mathbf{h}}_{k,j,1}^H}{\frac{1}{N^2} \|\hat{\mathbf{h}}_{k,j,1}\|^4} \right. \\ &\quad \left. - 2\Re \left[\frac{(\frac{1}{N} \mathbf{v}_{k,j,1} \hat{\mathbf{h}}_{k,j,1}^H)^* \frac{1}{N} \mathbf{v}_{k,j,1} \mathbf{Q}_{k,j}^{11} \hat{\mathbf{h}}_{k,j,1}^H}{\frac{1}{N} \|\hat{\mathbf{h}}_{k,j,1}\|^2} \right] \right). \end{aligned}$$

Since $\mathbf{v}_{k,j,1}$ and $\hat{\mathbf{h}}_{k,j,1}$ are independent, the second and third term in the bracket converge to 0. It can be shown that

$$\frac{1}{N} \mathbf{v}_{k,j,1} \mathbf{Q}_{k,j}^{11} \mathbf{v}_{k,j,1}^H - \frac{1}{1 + \epsilon} \left[g(\beta, \bar{\rho}) + \bar{\rho} \frac{\partial}{\partial \bar{\rho}} g(\beta, \bar{\rho}) \right] \xrightarrow{i.p.} 0.$$

The large system limit for the last term of $E_{k,j}$ can be done in the same way. Thus,

$$E_{k,j} - \frac{2^{-\bar{B}_d} + \epsilon 2^{-\bar{B}_c}}{1 + \epsilon} \left[g(\beta, \bar{\rho}) + \bar{\rho} \frac{\partial}{\partial \bar{\rho}} g(\beta, \bar{\rho}) \right] \xrightarrow{i.p.} 0.$$

7) c^2 : We can show that

$$c^2 - \frac{\frac{1}{2} P_t (1 + \epsilon)}{g(\beta, \bar{\rho}) + \bar{\rho} \frac{\partial}{\partial \bar{\rho}} g(\beta, \bar{\rho})} \xrightarrow{a.s.} 0.$$

Since $\xrightarrow{a.s.}$ implies $\xrightarrow{i.p.}$ then c^2 also converges weakly to the same quantity as above.

Combining the results, it follows that the signal strength and the interference converge to

$$\frac{P(1+\epsilon)d^2g^2(\beta, \bar{\rho})}{(1+g(\beta, \bar{\rho}))^2 \left(g(\beta, \bar{\rho}) + \bar{\rho} \frac{\partial}{\partial \bar{\rho}} g(\beta, \bar{\rho}) \right)} \quad (55)$$

and

$$P(1+\epsilon) \left(1 - \frac{d^2g(\beta, \bar{\rho})(2+g(\beta, \bar{\rho}))}{(1+g(\beta, \bar{\rho}))^2} \right), \quad (56)$$

respectively. Therefore, (26) follows immediately with $\rho_{M,Q} = \bar{\rho}$.

APPENDIX III

LARGE SYSTEM RESULTS FOR THE COORDINATED BEAMFORMING

For brevity in the proofs, we define the following (see also [17])

$$\begin{aligned} \mathbf{A}_j &= \left(\rho + \frac{1}{N} \sum_{m=1}^2 \sum_{l=1}^K \hat{\mathbf{h}}_{l,m,j}^H \hat{\mathbf{h}}_{l,m,j} \right)^{-1} \\ \mathbf{A}_{kj} &= \left(\rho + \frac{1}{N} \sum_{(l,m) \neq (k,j)} \hat{\mathbf{h}}_{l,m,j}^H \hat{\mathbf{h}}_{l,m,j} \right)^{-1} \\ \mathbf{A}_{kj,k'j',j} &= \left(\rho + \frac{1}{N} \sum_{(l,m) \neq (k,j), (k',j')} \hat{\mathbf{h}}_{l,m,j}^H \hat{\mathbf{h}}_{l,m,j} \right)^{-1}. \end{aligned}$$

From the definitions above, we can write the numerator of the SINR_{k,j} (3) excluding c_j^2 , as follows

$$\begin{aligned} |\mathbf{h}_{k,j,j} \mathbf{w}_{kj}|^2 &= \left| \frac{\sqrt{\phi_{k,j,j}}}{N} \hat{\mathbf{h}}_{k,j,j} \mathbf{A}_{kj} \hat{\mathbf{h}}_{k,j,j}^H \right|^2 + \left| \frac{1}{N} \tilde{\mathbf{h}}_{k,j,j} \mathbf{A}_{kj} \hat{\mathbf{h}}_{k,j,j}^H \right|^2 \\ &\quad + 2\Re \left[\frac{1}{N^2} (\tilde{\mathbf{h}}_{k,j,j} \mathbf{A}_{kj} \hat{\mathbf{h}}_{k,j,j}^H) (\hat{\mathbf{h}}_{k,j,j} \mathbf{A}_{kj} \hat{\mathbf{h}}_{k,j,j}^H) \right] = \phi_{k,j,j} |S_{kj}^{(1)}|^2 + |S_{kj}^{(2)}|^2 + S_{kj}^{(3)}. \end{aligned}$$

In denominator, let us consider the term $|\mathbf{h}_{k,j,j'} \mathbf{w}_{k'j'}|^2$ which can be expanded as follows

$$|\mathbf{h}_{k,j,j'} \mathbf{w}_{k'j'}|^2 = \frac{1}{N^2} \phi_{k,j,j'} \hat{\mathbf{h}}_{k,j,j'} \mathbf{A}_{k'j'} \hat{\mathbf{h}}_{k',j',j'}^H \hat{\mathbf{h}}_{k',j',j'} \mathbf{A}_{k'j'} \hat{\mathbf{h}}_{k,j,j'}^H + \frac{1}{N^2} \tilde{\mathbf{h}}_{k,j,j'} \mathbf{A}_{k'j'} \hat{\mathbf{h}}_{k',j',j'}^H \hat{\mathbf{h}}_{k',j',j'} \mathbf{A}_{k'j'} \tilde{\mathbf{h}}_{k,j,j'}^H \quad (57)$$

$$- 2\Re \left[\frac{\sqrt{\phi_{k,j,j'}}}{N^2} \tilde{\mathbf{h}}_{k,j,j'} \mathbf{A}_{k'j'} \hat{\mathbf{h}}_{k',j',j'}^H \hat{\mathbf{h}}_{k',j',j'} \mathbf{A}_{k'j'} \hat{\mathbf{h}}_{k,j,j'}^H \right] \quad (58)$$

$$= \frac{1}{N} I_{kj,k'j'}^{(1)} + \frac{1}{N} I_{kj,k'j'}^{(2)} - \frac{1}{N} I_{kj,k'j'}^{(3)} = \frac{1}{N} \mathcal{I}. \quad (59)$$

Now, we are going to derive the large system limit for $\frac{1}{N} \text{Tr}(\mathbf{A}_j)$ since it will be used frequently in this section.

Let $\hat{\mathbf{H}}_j = [\hat{\mathbf{h}}_{1,1,j} \ \cdots \ \hat{\mathbf{h}}_{K,1,j} \ \hat{\mathbf{h}}_{1,2,j} \ \cdots \ \hat{\mathbf{h}}_{K,2,j}]^T$ and $\hat{\mathbf{h}}_{k,i,j} \sim \mathcal{CN}(0, \omega_{ij} \mathbf{I})$. Then, $\mathbf{A}_j = \left(\rho + \frac{1}{N} \hat{\mathbf{H}}_j^H \hat{\mathbf{H}}_j \right)^{-1}$ and

$$\frac{1}{N} \text{Tr}(\mathbf{A}_j) = \int \frac{1}{\lambda + \rho} dF_{\hat{\mathbf{H}}_j^H \hat{\mathbf{H}}_j}$$

where $F_{\hat{\mathbf{H}}_j^H \hat{\mathbf{H}}_j}$ is the empirical eigenvalue distribution of $\hat{\mathbf{H}}_j^H \hat{\mathbf{H}}_j$. From Theorem 8, this distribution converges almost surely to a limiting distribution F whose Stieltjes transform $m_F(z)$. It can be shown that

$$\frac{1}{N} \text{Tr}(\mathbf{A}_j) \xrightarrow{a.s.} m_F(-\rho) = \int_0^1 u(x, -\rho) dx.$$

where

$$u(x, -\rho) = u(-\rho) = \frac{1}{\rho + \frac{\beta\omega_{1j}}{1+\omega_{1j}u(-\rho)} + \frac{\beta\omega_{2j}}{1+\omega_{2j}u(-\rho)}} = \frac{1}{\rho + \frac{\beta\omega_d}{1+\omega_d u(-\rho)} + \frac{\beta\omega_c}{1+\omega_c u(-\rho)}}.$$

for $0 \leq x \leq 1$. Let $\Gamma = u(-\rho)$, then $\frac{1}{N} \text{Tr}(\mathbf{A}_j) \xrightarrow{a.s.} \Gamma$.

A. Analog Feedback

Based on the channel model (1), we have $\phi_{k,j,j} = \phi_{k,j,j'} = 1$. The definitions for other terms such as ω_\bullet and δ_\bullet can be seen in Section II-C. Now, let us first derive the large system limit for the numerator of the SINR $_{kj}$. We start with the term $S_{kj}^{(1)}$. From Lemma 1 and by applying [42, Lemma 5.1], we can show that

$$\max_{j=1,2,k \leq K} \left| S_{kj}^{(1)} - \frac{\omega_d}{N} \text{Tr}(\mathbf{A}_{kj}) \right| \xrightarrow{a.s.} 0.$$

By applying rank-1 perturbation lemma (see e.g., [17, Lemma 3], [43, Lemma 14.3]), we have

$$\max_{j=1,2,k \leq K} \left| S_{kj}^{(1)} - \frac{\omega_d}{N} \text{Tr}(\mathbf{A}_j) \right| \xrightarrow{a.s.} 0$$

where $\frac{1}{N} \text{Tr}(\mathbf{A}_j) \xrightarrow{a.s.} \Gamma$.

Since $\hat{\mathbf{h}}_{k,j,j}$, \mathbf{A}_{kj} and $\tilde{\mathbf{h}}_{k,j,j}$ are independent then it follows that

$$\max_{j=1,2,k \leq K} \left| \tilde{\mathbf{h}}_{k,j,j} \mathbf{A}_{kj} \hat{\mathbf{h}}_{k,j,j}^H \right| \xrightarrow{a.s.} 0.$$

Consequently,

$$\max_{j=1,2,k \leq K} \left| S_{kj}^{(2)} \right| \xrightarrow{a.s.} 0 \text{ and } \max_{j=1,2,k \leq K} \left| S_{kj}^{(3)} \right| \xrightarrow{a.s.} 0.$$

In summary,

$$\max_{j=1,2,k \leq K} \left| |\mathbf{h}_{k,j,j} \mathbf{w}_{kj}|^2 - \omega_d^2 \Gamma^2 \right| \xrightarrow{a.s.} 0.$$

Now, let us move in analyzing the interference term. By using the matrix inversion lemma, we can rewrite $I_{kj,k'j'}^{(1)}$ as

$$I_{kj,k'j'}^{(1)} = \frac{\frac{1}{N} \phi_{k,j,j'} \hat{\mathbf{h}}_{k,j,j'} \mathbf{A}_{k'j',kj,j'} \hat{\mathbf{h}}_{k',j',j'}^H \hat{\mathbf{h}}_{k',j',j'} \mathbf{A}_{k'j',kj,j'} \hat{\mathbf{h}}_{k,j,j'}^H}{\left(1 + \frac{1}{N} \hat{\mathbf{h}}_{k,j,j'} \mathbf{A}_{k'j',kj,j'} \hat{\mathbf{h}}_{k,j,j'}^H \right)^2}.$$

By applying Lemma 1, [42, Lemma 5.1] and rank-1 perturbation lemma (R1PL) twice, we can show

$$\max_{j,j'=1,2,k,k' \leq K, (k,j) \neq (k',j')} \left| \frac{1}{N} \hat{\mathbf{h}}_{k,j,j'} \mathbf{A}_{k'j',kj,j'} \hat{\mathbf{h}}_{k,j,j'}^H - \frac{\omega_{jj'}}{N} \text{Tr}(\mathbf{A}_{j'}) \right| \xrightarrow{a.s.} 0.$$

Similarly,

$$\max_{j,j'=1,2,k,k'\leq K, (k,j)\neq(k',j')} \left| \frac{1}{N} \hat{\mathbf{h}}_{k,j,j'} \mathbf{A}_{k'j',k,j,j'} \hat{\mathbf{h}}_{k',j',j'}^H \hat{\mathbf{h}}_{k',j',j'} \mathbf{A}_{k'j',k,j,j'} \hat{\mathbf{h}}_{k,j,j'}^H - \frac{\omega_{jj'}\omega_d}{N} \text{Tr}(\mathbf{A}_{j'}^2) \right| \xrightarrow{a.s.} 0.$$

Since $\frac{1}{N} \text{Tr}(\mathbf{A}_{j'}) \rightarrow \Gamma$ and $\frac{1}{N} \text{Tr}(\mathbf{A}_{j'}^2) \rightarrow -\frac{\partial \Gamma}{\partial \rho}$, we have

$$\max_{j,j'=1,2,k,k'\leq K, (k,j)\neq(k',j')} \left| I_{kj,k'j'}^{(1)} - \omega_d \left(-\frac{\omega_{jj'}}{(1+\omega_{jj'}\Gamma)^2} \frac{\partial \Gamma}{\partial \rho} \right) \right| \xrightarrow{a.s.} 0.$$

By following the same steps, we obtain

$$\max_{j,j'=1,2,k,k'\leq K, (k,j)\neq(k',j')} \left| I_{kj,k'j'}^{(2)} - \left(-\delta_{jj'}\omega_d \frac{\partial \Gamma}{\partial \rho} \right) \right| \xrightarrow{a.s.} 0.$$

and

$$\max_{j,j'=1,2,k,k'\leq K, (k,j)\neq(k',j')} \left| I_{kj,k'j'}^{(3)} \right| \xrightarrow{a.s.} 0.$$

Combining the results, we have the large system limit for \mathcal{I} in (59)

$$\max_{j,j'=1,2,k,k'\leq K, (k,j)\neq(k',j')} \left| \mathcal{I} - \omega_d \left(-\frac{\omega_{jj'}}{(1+\omega_{jj'}\Gamma)^2} - \delta_{jj'} \right) \frac{\partial \Gamma}{\partial \rho} \right| \xrightarrow{a.s.} 0. \quad (60)$$

Using (60), the large system result for the interference term can be written as follows

$$\begin{aligned} \sum_{(k',j')\neq(k,j)} |\mathbf{h}_{k,j,j'} \mathbf{w}_{k'j'}|^2 &= \sum_{l=1, l\neq k}^K |\mathbf{h}_{k,j,j} \mathbf{w}_{lj}|^2 + \sum_{l=1}^K |\mathbf{h}_{k,j,\bar{j}} \mathbf{w}_{l\bar{j}}|^2 \\ &\xrightarrow{a.s.} -\beta\omega_d \left(\frac{\omega_d}{(1+\omega_d\Gamma)^2} + \frac{\omega_c}{(1+\omega_c\Gamma)^2} + \delta_d + \delta_c \right) \frac{\partial \Gamma}{\partial \rho}. \end{aligned}$$

Now, we just need to derive the large system limit for $c_j^2 = P \left(\sum_{k=1}^K \|\mathbf{w}_{kj}\|^2 \right)^{-1}$, where we can express $\|\mathbf{w}_{kj}\|^2 = \frac{1}{N^2} \hat{\mathbf{h}}_{k,j,j} \mathbf{A}_{kj}^2 \hat{\mathbf{h}}_{k,j,j}^H$. We can show that

$$\max_{j=1,2,k\leq K} \left| \frac{1}{N^2} \hat{\mathbf{h}}_{k,j,j} \mathbf{A}_{kj}^2 \hat{\mathbf{h}}_{k,j,j}^H - \frac{\omega_d}{N} \text{Tr}(\mathbf{A}_j^2) \right| \xrightarrow{a.s.} 0.$$

Thus,

$$c_j^2 \xrightarrow{a.s.} \frac{P}{-\beta\omega_d \frac{\partial \Gamma}{\partial \rho}},$$

where we can show that

$$-\frac{\partial \Gamma}{\partial \rho} = -\Gamma' = \frac{\Gamma}{\rho + \frac{\beta\omega_c}{(1+\omega_c\Gamma)^2} + \frac{\beta\omega_d}{(1+\omega_d\Gamma)^2}}. \quad (61)$$

To sum up, from the analyses above, we can express the limiting signal energy as

$$\frac{1}{\beta} P \omega_d \Gamma \left(\rho + \frac{\beta\omega_c}{(1+\omega_c\Gamma)^2} + \frac{\beta\omega_d}{(1+\omega_d\Gamma)^2} \right) \quad (62)$$

and the limiting interference energy as

$$P \left(\frac{\omega_d}{(1 + \omega_d \Gamma)^2} + \frac{\omega_c}{(1 + \omega_c \Gamma)^2} + \delta_d + \delta_c \right) \quad (63)$$

Finally, the limiting SINR can be expressed as (21), with $\Gamma_A = \Gamma$ and $\rho_{\text{C,AF}} = \rho$.

B. Proof of Theorem 6: Quantized Feedback via RVQ

In the derivation of the large system limit SINR in this section, we use some of the results presented in the previous section. Here, we have $\omega_{jj} = \omega_d = 1$ and $\omega_{j\bar{j}} = \omega_c = \epsilon$. From (1), we have $\phi_{k,j,i} = 1 - \tau_{k,j,i}^2$.

First, let us consider the numerator of the SINR. By using the result from previous section, we have

$$\max_{j=1,2,k \leq K} \left| S_{kj}^{(1)} - \frac{1}{N} \text{Tr}(\mathbf{A}_j) \right| \xrightarrow{a.s.} 0$$

where $\frac{1}{N} \text{Tr}(\mathbf{A}_j) \xrightarrow{a.s.} \Gamma$ and Γ is the solution of

$$\Gamma = \frac{1}{\rho + \frac{\beta}{1+\Gamma} + \frac{\beta\epsilon}{1+\epsilon\Gamma}}.$$

As stated in [16], we have,

$$\phi_{k,j,j} \xrightarrow{L_2} 1 - 2^{-\bar{B}_d}. \quad (64)$$

Since almost sure convergence and convergence in mean square imply the convergence in probability then

$$\phi_{k,j,j} |S_{kj}^{(1)}|^2 - (1 - 2^{-\bar{B}_d}) \Gamma^2 \xrightarrow{i.p.} 0.$$

By using (8), the term $\tilde{\mathbf{h}}_{k,j,j} \mathbf{A}_{kj} \hat{\mathbf{h}}_{k,j,j}^H$ in $S_{kj}^{(3)}$ can be rewritten as

$$\begin{aligned} \frac{1}{N} \tilde{\mathbf{h}}_{k,j,j} \mathbf{A}_{kj} \hat{\mathbf{h}}_{k,j,j}^H &= \frac{\tau_{k,j,j} \|\mathbf{h}_{k,j,j}\|}{\|\mathbf{v}_{k,j,j} \mathbf{\Pi}_{\hat{\mathbf{h}}_{k,j,j}}^\perp\|} \left(\frac{1}{N} \mathbf{v}_{k,j,j} \mathbf{\Pi}_{\hat{\mathbf{h}}_{k,j,j}}^\perp \hat{\mathbf{h}}_{k,j,j}^H \right) \\ &= \frac{\tau_{k,j,j} \|\mathbf{h}_{k,j,j}\|}{\|\mathbf{v}_{k,j,j} \mathbf{\Pi}_{\hat{\mathbf{h}}_{k,j,j}}^\perp\|} \left(\frac{1}{N} \mathbf{v}_{k,j,j} \mathbf{A}_{kj} \hat{\mathbf{h}}_{k,j,j}^H - \frac{(\frac{1}{N} \mathbf{v}_{k,j,j} \hat{\mathbf{h}}_{k,j,j}^H) \hat{\mathbf{h}}_{k,j,j} \mathbf{A}_{kj} \hat{\mathbf{h}}_{k,j,j}^H}{\|\hat{\mathbf{h}}_{k,j,j}\|^2} \right). \end{aligned}$$

Since $\mathbf{v}_{k,j,j}$ and $\hat{\mathbf{h}}_{k,j,j}^H$ are independent, then

$$\max_{j=1,2,k \leq K} \left| \frac{1}{N} \mathbf{v}_{k,j,j} \hat{\mathbf{h}}_{k,j,j}^H \right| \xrightarrow{a.s.} 0, \text{ and } \max_{j=1,2,k \leq K} \left| \frac{1}{N} \mathbf{v}_{k,j,j} \mathbf{A}_{kj} \hat{\mathbf{h}}_{k,j,j}^H \right| \xrightarrow{a.s.} 0.$$

It can also be shown that

$$\max_{j=1,2,k \leq K} \left| \frac{1}{N} \|\mathbf{h}_{k,j,j}\|^2 - 1 \right| \xrightarrow{a.s.} 0, \text{ and } \max_{j=1,2,k \leq K} \left| \frac{1}{N} \|\mathbf{v}_{k,j,j} \mathbf{\Pi}_{\hat{\mathbf{h}}_{k,j,j}}^\perp\|^2 - 1 \right| \xrightarrow{a.s.} 0.$$

Hence,

$$\frac{1}{N} \tilde{\mathbf{h}}_{k,j,j} \mathbf{A}_{kj} \hat{\mathbf{h}}_{k,j,j}^H \xrightarrow{i.p.} 0, \quad (65)$$

and thus,

$$S_{kj}^{(2)} \xrightarrow{i.p.} 0, \text{ and } S_{kj}^{(3)} \xrightarrow{i.p.} 0.$$

Putting the results together, we have the following for the numerator

$$|\mathbf{h}_{k,j,j} \mathbf{w}_{k,j}|^2 - (1 - 2^{-\bar{B}_d}) \Gamma^2 \xrightarrow{i.p.} 0.$$

Now, let us consider the interference terms. By using the same steps as in the previous section, we can show the followings

$$\begin{aligned} \max_{j,j'=1,2,k,k' \leq K, (k,j) \neq (k',j')} \left| I_{kj,k'j'}^{(1)} - \left(-\frac{(1 - 2^{-\bar{B}_{jj'}}) \omega_{jj'}}{(1 + \omega_{jj'} \Gamma)^2} \frac{\partial \Gamma}{\partial \rho} \right) \right| &\xrightarrow{i.p.} 0, \\ \max_{j,j'=1,2,k,k' \leq K, (k,j) \neq (k',j')} \left| I_{kj,k'j'}^{(2)} - \epsilon_{jj'} 2^{-\bar{B}_{jj'}} \frac{\partial \Gamma}{\partial \rho} \right| &\xrightarrow{i.p.} 0, \end{aligned}$$

and

$$\max_{j,j'=1,2,k,k' \leq K, (k,j) \neq (k',j')} |I_{kj,k'j'}^{(3)}| \xrightarrow{i.p.} 0,$$

where $\bar{B}_{jj'} = \bar{B}_d$ when $j = j'$ and otherwise $\bar{B}_{jj'} = \bar{B}_c$.

Combining the results, we have

$$\max_{j,j'=1,2,k,k' \leq K, (k,j) \neq (k',j')} \left| \mathcal{I} - \left(-\frac{(1 - 2^{-\bar{B}_{jj'}}) \omega_{jj'}}{(1 + \omega_{jj'} \Gamma)^2} - \epsilon_{jj'} 2^{-\bar{B}_{jj'}} \right) \frac{\partial \Gamma}{\partial \rho} \right| \xrightarrow{i.p.} 0. \quad (66)$$

Using (66), the large system result for the interference term can be written as follows

$$\begin{aligned} \sum_{(k',j') \neq (k,j)} |\mathbf{h}_{k,j,j'} \mathbf{w}_{k',j'}|^2 &= \sum_{l=1, l \neq k}^K |\mathbf{h}_{k,j,j} \mathbf{w}_{lj}|^2 + \sum_{l=1}^K |\mathbf{h}_{k,j,j} \mathbf{w}_{lj}|^2 \\ &\xrightarrow{i.p.} -\beta \left(\frac{1 - 2^{-\bar{B}_d}}{(1 + \Gamma)^2} + \frac{\epsilon(1 - 2^{-\bar{B}_c})}{(1 + \epsilon \Gamma)^2} + 2^{-\bar{B}_d} + \epsilon 2^{-\bar{B}_c} \right) \frac{\partial \Gamma}{\partial \rho}. \end{aligned}$$

By using the result from the previous results straightforwardly, we have $c_j^2 \xrightarrow{a.s.} \frac{P}{-\beta \frac{\partial \Gamma}{\partial \rho}}$. Putting all the large system results for each term, we can show that the limiting signal strength is

$$\frac{1}{\beta} P \phi_d \Gamma \left(\rho + \frac{\beta \epsilon}{(1 + \epsilon \Gamma)^2} + \frac{\beta}{(1 + \Gamma)^2} \right) \quad (67)$$

and the limiting interference energy becomes

$$P \left(\frac{\phi_d}{(1 + \Gamma)^2} + \frac{\epsilon \phi_c}{(1 + \epsilon \Gamma)^2} + \delta_d + \delta_c \right). \quad (68)$$

Let $\rho_{c,Q} = \rho$ and $\Gamma_Q = \Gamma$. Then, we can obtain the limiting SINR given by (35) from (67) and (68) straightforwardly.

REFERENCES

- [1] D. Gesbert, S. Hanly, H. Huang, S. Shamai Shitz, O. Simeone, and W. Yu, "Multi-cell MIMO cooperative networks: A new look at interference," *IEEE Journal on Selected Areas in Communications*, vol. 28, no. 9, pp. 1380–1408, 2010.
- [2] R. Bhagavatula and R. W. Heath, "Adaptive limited feedback for sum-rate maximizing beamforming in cooperative multicell systems," *IEEE Transactions on Signal Processing*, vol. 59, no. 2, pp. 800–811, 2011.
- [3] S. Shamai and B. Zaidel, "Enhancing the cellular downlink capacity via co-processing at the transmitting end," in *53rd IEEE Vehicular Technology Conference*, vol. 3, 2001, pp. 1745–1749 vol.3.
- [4] H. Zhang and H. Dai, "Cochannel interference mitigation and cooperative processing in downlink multicell multiuser MIMO networks," *Eurasip Journal on Wireless Communications and Networking*, vol. 2004, no. 2, pp. 222–235, December 2004.
- [5] M. Karakayali, G. Foschini, and R. Valenzuela, "Network coordination for spectrally efficient communications in cellular systems," *IEEE Wireless Communications Magazine*, vol. 13, no. 4, pp. 56–61, 2006.
- [6] G. Foschini, K. Karakayali, and R. Valenzuela, "Coordinating multiple antenna cellular networks to achieve enormous spectral efficiency," *IEEE Proceedings Communications*, vol. 153, no. 4, pp. 548–555, 2006.
- [7] S. Jing, D. N. C. Tse, J. B. Soriaga, J. Hou, J. E. Smee, and R. Adovani, "Multicell downlink capacity with coordinated processing," *EURASIP Journal on Wireless Communications and Networking*, vol. 2008, pp. 1–19, 2008.
- [8] O. Somekh, O. Simeone, Y. Bar-Ness, A. Haimovich, and S. Shamai, "Cooperative multicell zero-forcing beamforming in cellular downlink channels," *IEEE Transactions on Information Theory*, vol. 55, no. 7, pp. 3206–3219, July 2009.
- [9] A. Goldsmith, S. A. Jafar, N. Jindal, and S. Vishwanath, "Capacity limits of MIMO channels," *IEEE Journal on Selected Areas in Communications*, vol. 21, no. 5, pp. 684–702, 2003.
- [10] E. Biglieri, R. Calderbank, A. Costantinides, A. Goldsmith, and A. Paulraj, *MIMO Wireless Communications*. New York: Cambridge University Press, 2007.
- [11] D. J. Love, R. W. Heath, V. K. N. Lau, D. Gesbert, B. D. Rao, and M. Andrews, "An overview of limited feedback in wireless communication systems," *IEEE Journal on Selected Areas in Communications*, vol. 26, no. 8, pp. 1341–1365, 2008.
- [12] S. A. Ramprasad and G. Caire, "Cellular vs. network MIMO: A comparison including the channel state information overhead," in *Proc. IEEE 20th Int Personal, Indoor and Mobile Radio Communications Symp*, 2009, pp. 878–884.
- [13] S. A. Ramprasad, G. Caire, and H. C. Papadopoulos, "Cellular and network MIMO architectures: MU-MIMO spectral efficiency and costs of channel state information," in *Proc. Conf Signals, Systems and Computers Record of the Forty-Third Asilomar Conf*, 2009, pp. 1811–1818.
- [14] J. Zhang, J. G. Andrews, and K. B. Letaief, "Spatial intercell interference cancellation with CSI training and feedback," *IEEE Transaction on Wireless Communications*, May 2011, submitted. [Online]. Available: <http://arxiv.org/pdf/1105.4206>
- [15] T. L. Marzetta and B. M. Hochwald, "Fast transfer of channel state information in wireless systems," *IEEE Transactions on Signal Processing*, vol. 54, no. 4, pp. 1268–1278, 2006.
- [16] W. Santipach and M. L. Honig, "Capacity of a multiple-antenna fading channel with a quantized precoding matrix," *IEEE Transactions on Information Theory*, vol. 55, no. 3, pp. 1218–1234, 2009.
- [17] R. Zakhour and S. Hanly, "Base Station Cooperation on the Downlink: Large System Analysis," *IEEE Transactions on Information Theory*, vol. 58, no. 4, pp. 2079–2106, April 2012.
- [18] R. Muharar, R. Zakhour, and J. Evans, "Base Station Cooperation with Noisy Analog Channel Feedback: A Large System Analysis," in *Proc. Int. Conf. Commun. (ICC)*, Ottawa, Canada, June 2012.
- [19] —, "Base Station Cooperation with Limited Feedback: A Large System Analysis," in *Proc. Int. Symp. Inform. Theory (ISIT)*, Cambridge, MA, July 2012.
- [20] N. Jindal, "MIMO broadcast channels with finite-rate feedback," *IEEE Transactions on Information Theory*, vol. 52, no. 11, pp. 5045–5060, 2006.

- [21] G. Caire, N. Jindal, M. Kobayashi, and N. Ravindran, "Multiuser MIMO achievable rates with downlink training and channel state feedback," *IEEE Transactions on Information Theory*, vol. 56, no. 6, pp. 2845–2866, 2010.
- [22] D. Samardzija and N. Mandayam, "Unquantized and uncoded channel state information feedback in multiple-antenna multiuser systems," *IEEE Transactions on Communications*, vol. 54, no. 7, pp. 1335–1345, 2006.
- [23] M. Kobayashi, N. Jindal, and G. Caire, "Training and feedback optimization for multiuser MIMO downlink," *IEEE Transactions on Communications*, vol. 59, no. 8, pp. 2228–2240, 2011.
- [24] S. Wagner, R. Couillet, M. Debbah, and D. T. M. Slock, "Large System Analysis of Linear Precoding in Correlated MISO Broadcast Channels Under Limited Feedback," *IEEE Transactions on Information Theory*, vol. 58, no. 7, pp. 4509–4537, July 2012.
- [25] H. Huh, A. Tulino, and G. Caire, "Network MIMO With Linear Zero-Forcing Beamforming: Large System Analysis, Impact of Channel Estimation, and Reduced-Complexity Scheduling," *IEEE Transactions on Information Theory*, vol. 58, no. 5, pp. 2911–2934, May 2012.
- [26] J. Jose, A. Ashikhmin, T. L. Marzetta, and S. Vishwanath, "Pilot contamination and precoding in multi-cell TDD systems," *IEEE Transactions on Wireless Communications*, vol. 10, no. 8, pp. 2640–2651, 2011.
- [27] A. M. Tulino and S. Verdu, "Random matrix theory and wireless communications," *Foundations and Trends in Communications and Information Theory*, vol. 1, no. 1, 2004.
- [28] V. K. Nguyen and J. S. Evans, "Multiuser transmit beamforming via regularized channel inversion: A large system analysis," in *IEEE Globecom conference*, December 2008.
- [29] R. Muharar and J. Evans, "Optimal training for time-division duplexed systems with transmit beamforming," in *Proc. Australian Communications Theory Workshop (AusCTW)*, 2011, pp. 158–163.
- [30] —, "Downlink beamforming with transmit-side channel correlation: A large system analysis," in *Proc. IEEE Int Communications (ICC) Conf*, 2011, pp. 1–5.
- [31] C. B. Peel, B. M. Hochwald, and A. L. Swindlehurst, "A vector-perturbation technique for near-capacity multiantenna multiuser communication-part i: channel inversion and regularization," *IEEE Transactions on Communications*, vol. 53, no. 1, pp. 195–202, 2005.
- [32] N. Ravindran and N. Jindal, "Multi-user diversity vs. accurate channel feedback for MIMO broadcast channels," in *Proc. IEEE Int. Conf. Communications ICC '08*, 2008, pp. 3684–3688.
- [33] C. K. Au-Yeung and D. J. Love, "On the performance of random vector quantization limited feedback beamforming in a MISO system," *IEEE Transactions on Wireless Communications*, vol. 6, no. 2, pp. 458–462, 2007.
- [34] N. Jindal, "Antenna combining for the MIMO downlink channel," *IEEE Transactions on Wireless Communications*, vol. 7, no. 10, pp. 3834–3844, 2008.
- [35] D. Tse and S. Hanly, "Linear multiuser receivers: effective interference, effective bandwidth and user capacity," *Information Theory, IEEE Transactions on*, vol. 45, no. 2, pp. 641–657, mar 1999.
- [36] A. W. van der Vaart, *Asymptotic Statistics*, ser. Cambridge series in statistical and probabilistic mathematics. Cambridge University Press, 1998.
- [37] V. K. Nguyen, R. Muharar, and J. Evans, "Multiuser transmit beamforming via regularized channel inversion: A large system analysis," Tech. Rep., November 2009. [Online]. Available: <http://cubinlab.ee.unimelb.edu.au/~rmuharar>
- [38] W. Santipach and M. L. Honig, "Optimization of training and feedback overhead for beamforming over block fading channels," *IEEE Transactions on Information Theory*, vol. 56, no. 12, pp. 6103–6115, 2010.
- [39] E. Larsson and P. Stoica, *Space-Time Block Coding for Wireless Communications*. Cambridge University Press, 2003.
- [40] J. Evans and D. N. C. Tse, "Large system performance of linear multiuser receivers in multipath fading channels," *IEEE Transactions on Information Theory*, vol. 46, no. 6, pp. 2059–2078, 2000.
- [41] S. V. Hanly and D. N. C. Tse, "Resource pooling and effective bandwidths in CDMA networks with multiuser receivers and spatial diversity," *IEEE Transactions on Information Theory*, vol. 47, no. 4, pp. 1328–1351, 2001.

- [42] Y.-C. Liang, G. Pan, and Z. D. Bai, "Asymptotic performance of MMSE receivers for large systems using random matrix theory," *IEEE Transactions on Information Theory*, vol. 53, no. 11, pp. 4173–4190, 2007.
- [43] R. Couillet and M. Debbah, *Random Matrix Methods for Wireless Communications*. Cambridge University Press, 2011.